Evaluation of operational online-coupled regional air quality models over Europe and North America in the context of AQMEII phase 2. Part II: Particulate Matter

Ulas Im[a], Roberto Bianconi[b], Efisio Solazzo[a], Ioannis Kioutsioukis[a], Alba Badia[c], Alessandra Balzarini[d], Rocío Baró[e], Roberto Bellasio[b], Dominik Brunner[f], Charles Chemel[g], Gabriele Curci[h], Hugo Denier van der Gon[i], Johannes Flemming[j], Renate Forkel[k], Lea Giordano[f], Pedro Jiménez-Guerrero[e], Marcus Hirtl[l], Alma Hodzic[m], Luka Honzak[n], Oriol Jorba[c], Christoph Knote[m], Paul A. Makar[o], Astrid Manders-Groot[i], Lucy Neal[p], Juan L. Pérez[q], Guidio Pirovano[d], George Pouliot[r], Roberto San Jose[q], Nicholas Savage[p], Wolfram Schroder[s], Ranjeet S. Sokhi[g], Dimiter Syrakov[t], Alfreida Torian[r], Paolo Tuccella[h], Kai Wang[u], Johannes Werhahn[k], Ralf Wolke[s], Rahela Zabkar[n,v], Yang Zhang[u], Junhua Zhang[o], Christian Hogrefe[r], Stefano Galmarini[a*]

a. European Commission, Joint Research Centre, Institute for Environment and Sustainability, Air and Climate Unit, Ispra (Italy).
b. Enviroware srl, Concorezzo (MB), Italy.
c. Earth Sciences Department, Barcelona Supercomputing Center (BSC-CNS), Barcelona, Spain.
d. Ricerca sul Sistema Energetico (RSE SpA), Milano, Italy
e. University of Murcia, Department of Physics, Physics of the Earth. Campus de Espinardo, Ed. CIOyN, 30100 Murcia, Spain.
f. Laboratory for Air Pollution and Environmental Technology, Empa, Dubendorf, Switzerland.
g. Centre for Atmospheric & Instrumentation Research, University of Hertfordshire, College Lane, Hatfield, AL10 9AB, UK.
h. Department of Physical and Chemical Sciences, Center of Excellence for the forecast of Severe Weather (CETEMPS), University of L'Aquila, L'Aquila, Italy.
i. Netherlands Organization for Applied Scientific Research (TNO), Utrecht, The Netherlands.
j. ECMWF, Shinfield Park, RG2 9AX Reading, United Kingdom.
k. Karlsruher Institut für Technologie (KIT), Institut für Meteorologie und Klimaforschung, Atmosphärische Umweltforschung (IMK-IFU), Kreuzeckbahnstr. 19, 82467 Garmisch-Partenkirchen, Germany.
l. Section Environmental Meteorology, Division Customer Service, ZAMG - Zentralanstalt für Meteorologie und Geodynamik, 1190 Wien, Austria.
m. National Center for Atmospheric Research, Boulder, CO, US.
n. Center of Excellence SPACE-SI, Ljubljana, Slovenia.
o. Air Quality Research Section, Atmospheric Science and Technology Directorate, Environment Canada, 4905 Dufferin Street, Toronto, Ontario, Canada.
p. Met Office, FitzRoy Road, Exeter, EX1 3PB, United Kingdom.
q. Environmental Software and Modelling Group, Computer Science School - Technical University of Madrid, Campus de Montegancedo - Boadilla del Monte-28660, Madrid, Spain.

r. Emissions and Model Evaluation Branch, Atmospheric Modeling and Analysis Division/NERL/ORD, Research Triangle Park, North Carolina, USA.
s. Leibniz Institute for Tropospheric Research, Permoserstr. 15, D-04318 Leipzig, Germany.
t. National Institute of Meteorology and Hydrology, Bulgarian Academy of Sciences, 66 Tzarigradsko shaussee Blvd., Sofia 1784, Bulgaria.
u. Department of Marine, Earth and Atmospheric Sciences, North Carolina State University, Raleigh, USA.
v. University of Ljubljana, Faculty of Mathematics and Physics, Ljubljana, Slovenia.

* Corresponding author: S. Galmarini (Stefano.galmarini@jrc.ec.europa.eu)

Highlights

- Seventeen modeling groups from EU and NA simulated PM for 2010 under AQMEII phase 2
- A general model underestimation of surface PM over both continents up to 80%
- Natural PM emissions may lead to large underestimations in simulated PM_{10}.
- Dry deposition can introduce large differences among models.

Keywords: AQMEII, on-line coupled models, performance analysis, particulate matter, Europe, North America

ABSTRACT

The second phase of the Air Quality Model Evaluation International Initiative (AQMEII) brought together seventeen modeling groups from Europe and North America, running eight operational online-coupled air quality models over Europe and North America using common emissions and boundary conditions. The simulated annual, seasonal, continental and sub-regional particulate matter (PM) surface concentrations for the year 2010 have been evaluated against a large observational database from different measurement networks operating in Europe and North America. The results show a systematic underestimation for all models in almost all seasons and sub-regions, with the largest underestimations for the Mediterranean region. The rural PM_{10} concentrations over Europe are underestimated by all models by up to 66% while the underestimations are much larger for the urban PM_{10} concentrations (up to 75%). On the other hand, there are overestimations in $PM_{2.5}$ levels suggesting that the large underestimations in the PM_{10} levels can be attributed to the natural dust emissions. Over North America, there is a general underestimation in PM_{10} in all seasons and sub-regions by up to ~90% due mainly to the underpredictions in soil dust. SO_4^{2-} levels over EU are underestimated by majority of the models while NO_3^- levels are largely overestimated, particularly in east and south Europe. NH_4^+ levels are also underestimated largely in south Europe. SO_4 levels over North America are particularly overestimated over the western US that is characterized by large anthropogenic emissions while the eastern USA is characterized by underestimated SO_4 levels by the majority of the models. Daytime AOD levels at 555nm is simulated within the 50% error range over both continents with differences attributed to differences in concentrations of the relevant species as well as in approaches in estimating the

AOD. Results show that the simulated dry deposition can lead to substantial differences among the models. Overall, the results show that representation of dust and sea-salt emissions can largely impact the simulated PM concentrations and that there are still major challenges and uncertainties in simulating the PM levels.

1. Introduction

Particulate matter (PM) is related to respiratory and cardiovascular diseases as well as to mortality (Schwartz et al., 1996; Bernard et al., 2001). PM has direct and indirect effects on climate (IPCC, 2007) and in turn, climate may have a significant impact on PM levels and composition (Jacob and Winner, 2009). PM has both anthropogenic and natural sources and are emitted as primary aerosols or are chemically formed from gaseous precursors in the atmosphere. PM levels are still a concern, particularly in the urban areas and its adverse effects on climate and health are expected to persist (Klimont et al., 2009; Winker et al., 2013). Due to the greater potential of $PM_{2.5}$ (PM with an aerodynamic diameter smaller than 2.5 μm) to cause adverse effects on public health compared to PM_{10} (PM with an aerodynamic diameter below 10 μm), $PM_{2.5}$ attracted more scientific attention that led to air quality model (AQM) development to focus more on this size of PM and its composition. PM can lead to reductions in radiation reaching the earth and therefore impact the temperature, wind speed and humidity, and it can also modify cloud droplet size and number (Baklanov et al., 2014; Brunner et al., 2014). On-line coupled AQMs can simulate the aerosol feedbacks on meteorology that can be important on a wide range of temporal and spatial scales (Zhang 2008; Grell and Baklanov, 2011).

The Air Quality Model Evaluation International Initiative (AQMEII) is designed to promote policy-relevant research on regional air quality model evaluation across the atmospheric modeling communities in Europe (EU) and North America (NA) through the exchange of information on current practices and the identification of research priorities (Galmarini and Rao, 2011). Standardized observations and model outputs were made available through the ENSEMBLE web-based system (http://ensemble2.jrc.ec.europa.eu/public/) that is hosted at the Joint Research Centre (JRC; Bianconi et al., 2004; Galmarini et al., 2012). The first phase of AQMEII focused on the evaluation of off-line atmospheric modelling systems against large sets of monitoring observations over Europe and North America for the year 2006 (Solazzo et al., 2012a,b and 2013; Vautard et al., 2012; Hogrefe et al., 2014). The results from this first phase demonstrated a large underestimation by all models throughout the year and a large variability among models in representing emissions, deposition and concentrations of PM and their composition (Solazzo et al., 2012b).

The second phase of AQMEII extends this model assessment to on-line air quality models. In this study, we analyze PM_{10} and $PM_{2.5}$ mass concentrations simulated by eight on-line-coupled models, which have been run by seventeen independent groups from Europe and North America (a companion study is devoted to the analyses of ozone, Im et al., 2014). The surface PM levels simulated by the individual models as well as their ensemble mean and

median are compared with the observational data provided by the ENSEMBLE system. As multi-model ensemble analyses is not the scope of this paper, further analyses have been performed by Kioutsioukis et al. (2014) for the EU case using the multi-model data presented in the present paper. The aim of the study is to evaluate the performances of widely used operational on-line coupled models in EU and NA in simulating PM and its chemical components on a sub-regional and seasonal basis employing an experimental set up with common anthropogenic emission and boundary conditions and thus, to identify areas of model improvements and the links to policy applications.

2. Materials and Methods

2.1. Models

In the context of AQMEII2, thirteen modeling groups from EU and four modeling groups from NA have submitted PM simulations for the year 2010 (Table 1). One European group (BG2) employed an off-line coupled model while the rest of the groups performed their simulations using their operational on-line models. Nine groups used WRF/CHEM model (Grell et al., 2005) and its variant (e.g. Wang et al., 2014), having different gas-phase mechanisms (see Table 1 in Im et al., 2014) but similar aerosol modules that employ different size distributions approaches (modal/bin) and inorganic/organic aerosol treatments as seen in Table 1. The IT2 simulation is performed with an experimental version of WRF/Chem v. 3.4, where the new secondary organic aerosol scheme VBS was coupled to the aerosol indirect effects modules. Therefore, the bias of IT2 run should not be regarded as the bias of the general WRF/Chem modeling system, but only of this particular version under development. The simulations were conducted for continental-scale domains of EU and NA covering continental U.S., southern Canada and northern Mexico (Fig.1). To facilitate the cross-comparison between models, the participating groups interpolated their model output to a common grid with 0.25˚ resolution for both continents. Model values at observation locations were extracted from the original model output files for comparison to observations (described below).

2.2. Emissions and Boundary Conditions

Standard anthropogenic emissions were provided by the TNO (Netherlands Organization for Applied Scientific Research) for EU (Kuenen et al., 2014) and by U.S. EPA (United States Environmental Protection Agency) and Environment Canada for NA (Pouliot et al., 2014). The NA emissions were processed by the US EPA for all models except for GEM-MACH, where a different grid projection required separate processing by Environment Canada. Different assumptions were used for snow reduction of fugitive dust emissions in these two efforts. More information on the implementation of these emissions is provided in Im et al. (2014). The spatial distribution of annually-integrated anthropogenic $PM_{2.5}$ emissions for EU and NA domains are depicted in Fig.1. Anthropogenic PM_{10} emissions per km^2 in NA (76 ktons km^{-2} yr^{-1}) are larger than those in EU (69 ktons km^{-2} yr^{-1}) while EU is characterized by larger $PM_{2.5}$ emissions density (49 ktons km^{-2} yr^{-1}) compared to NA (29 ktons km^{-2} yr^{-1}). EU

also has more than a factor of two larger NOx, NMVOC and NH_3 emission densities compared to NA (Im et al., 2014). Note that the emissions over the oceans represent those originating only from the maritime sector (Kuenen et al., 2014; Pouliot et al., 2014). Fig.1 also shows the monthly variation of $PM_{2.5}$ emissions over EU and NA. There is a clear seasonal variation in EU emissions. Spring season is characterized with the highest emissions in both domains. The PM speciation profiles for EU are based on Kulmala et al. (2011) while the temporal profiles for the EU anthropogenic emissions are based on Schaap et al. (2005). Each modeling group used their own biogenic (see Table 1 in Im et al., 2014), dust, and sea-salt emission modules in their operational model as seen in Table 1. Hourly biomass burning emissions were provided by Finnish Meteorological Institute (FMI) fire assimilation system (http://is4fires.fmi.fi/; Sofiev et al., 2009; Soares et al., 2014). 3-D daily chemical boundary conditions were provided by the ECMWF IFS-MOZART model (referred as MACC hereafter) run in the context of the MACC-II project (Monitoring Atmospheric Composition and Climate – Interim Implementation) on 3-hourly and 1.125˚ spatial resolution (Inness et al., 2013). The aerosol chemical species available in the reanalysis included sea-salt, dust, organic matter, black carbon and sulfate. However, following the AQMEII Phase 1 experience described in Schere et al. (2012), MACC-II sea-salt concentrations were not used as chemical boundary conditions for the NA domain.

2.3. Observations

Observations of hourly and daily rural and urban surface PM_{10} and $PM_{2.5}$ mass concentrations with a data availability of at least 75% from different measurement networks in EU (EMEP (European Monitoring and Evaluation Programme; http://www.emep.int/) and AirBase (European AQ database; http://acm.eionet.europa.eu/databases/airbase/)) and NA (the Canadian National Atmospheric Chemistry (NAtChem) Database and Analysis Facility operated by Environment Canada (http://www.ec.gc.ca/natchem/) that contains measurements from the Canadian National Air Pollution Surveillance Network (http://maps-cartes.ec.gc.ca/rnspa-naps/data.aspx), the Canadian Air and Precipitation Monitoring Network (http://www.ec.gc.ca/natchem/), the U.S. Clean Air Status and Trends Network (http://java.epa.gov/castnet/clearsession.do), the U.S. Interagency Monitoring of Protected Visual Environments Network (http://views.cira.colostate.edu/web/DataWizard/), and the U.S. Environmental Protection Agency's Air Quality System database for U.S. air quality data (http://www.epa.gov/ttn/airs/airsaqs/detaildata/downloadaqsdata.htm)) have been used in order to evaluate the model performances in simulating the surface PM concentrations in the two continents (Figure 1). Daily averages were calculated using the hourly observations from the station where daily measurements were not available and the analyses were performed on the daily averaged PM concentrations. Daily observations from 1525 stations (439 rural and 1076 urban) in EU and 469 stations (158 rural and 311 urban) in NA were used for PM_{10} comparisons. For $PM_{2.5}$, data from 517 stations in EU (139 rural and 378 urban) and 659 stations in NA (311 rural and 348 urban) were used. A geographical breakdown into three sub-regions for each continent that is similar to that in Solazzo et al. (2012) was applied, which is based on emission and climatological characteristics (Fig.1). The European sub-region EU1 can be characterized by north-western European sources with a transition climate between marine and continental and hosts 618 stations for PM_{10} (216rural and 402 urban) and

255 stations for $PM_{2.5}$ (66 rural and 189 urban). EU2 covers the north-eastern and central Europe sources as well as Germany with 433 stations for PM_{10} (124 rural and 309 urban) and 124 stations for $PM_{2.5}$ (21 rural and 103 urban). EU3 is characterized by the Mediterranean type climate and sources covering 375 stations for PM_{10} (92 rural and 283 urban) and 94 stations for $PM_{2.5}$ (44 rural and 50 urban). Sub-region NA1 consists of the arid southwestern part of the U.S. with the western slope of the Rocky mountains on the east and hosts 113 stations for PM_{10} (44 rural and 69 urban) and 70 stations for $PM_{2.5}$ (37 rural and 33 urban). NA2 covers the more humid south eastern U.S. with 45 stations for PM_{10} (17 rural and 28 urban) and 117 stations for $PM_{2.5}$ (52 rural and 65 urban). NA3 consists of the northeastern NA that is characterized by the highest emission sources in NA covering 64 stations for PM_{10} (11 rural and 53 urban) and 188 stations for $PM_{2.5}$ (78 rural and 110 urban).

2.4. Statistical analyses

A number of statistical parameters, including Pearson's correlation coefficient (*PCC*), root mean square error (*RMSE*); normalized mean standard error (*NMSE*) and normalized mean bias (*NMB*) are calculated (Im et al., 2014) in order to compare the individual model performances as well as the ensemble mean and median. The comparisons are performed individually for the two domains and their sub-regions for the whole simulation period and on a seasonal basis, in order to identify which regions and/or seasons have systematic errors.

3. Results and Discussion

3.1. PM_{10}

3.1.1. Seasonal and regional surface levels over Europe

Comparisons of observed and simulated annual and domain-averaged PM_{10} and $PM_{2.5}$ concentrations over the rural and urban monitoring stations in EU and NA are presented in Table 2. The temporal variation of the rural PM_{10} levels over EU are moderate-to-well-reproduced by the models (*PCC*=0.18-0.86), while the variations at urban sites were reproduced with slightly lower agreement (*PCC*=0.06-0.82). For both station types, the lowest correlations are calculated for DE4, ES1 and UK4 (*PCC*<0.25) while BG2 and UK5 well-captured the variation of PM_{10} with *PCC* larger than 0.75. The monthly time series plots presented in Fig.2 and 3 (upper panels) also show that particularly in winter, the monthly temporal variations were not captured by any of the models while they mainly follow the temporal evolution introduced by the MACC model that provides the chemical boundaries. The figures show that the majority of the models produced spring and autumn peaks, particularly for the rural stations while these are not observed in the measurements or the MACC model, suggesting that the anthropogenic PM emissions or the online-simulated natural dust emissions can be responsible for these peaks. Over EU, the rural PM_{10} concentrations are underestimated by all models from 10% (UK4) to 66% (IT2). The underestimations are much larger for the urban PM_{10} concentrations ranging from 43% (UK4) to 75% (IT2), suggesting that the urban emissions were not able to represent the actual

emissions, given the coarse resolution of the models. The underestimations are in all percentiles as can be seen in the box-and-whisker plots presented in Fig.4. The figure also shows that the variability in the models are is much lower compared to the observed variability except for UK4 for the rural levels, which has the lowest bias for both station types. The general tendency of all models to underestimate observed PM_{10} concentrations may be at least partially attributable to sub-grid scale effects since monitors may be located near hot spots and may introduce substantial horizontal gradients near such hot spot locations.

Regarding sub-regional rural PM_{10} levels, the highest biases are calculated for EU2 (*NMB*=-34% to -75%), which is characterized by large anthropogenic emissions while EU1 and EU3 have relatively smaller biases (-10% to -63% and -12% to -57%, respectively). The temporal variability is best captured for the sub-region EU1 with *PCC* values between 0.4 and 0.9 and lowest in the sub-region EU2 (*PCC*=0.2 to 0.9). Similar to the continental scale (EU0), in all sub-regions, the smallest biases are calculated for the UK4 model while the largest are calculated for the IT2 model. For the urban PM_{10} levels, EU2 and EU3 have the largest biases (up to -81%). UK4 model has the lowest *MNB* values while IT2 model is again associated with has the largest biases. The temporal variation was best reproduced by the UK5 model for all sub-regions except for EU3 where highest *PCC* is calculated for IT1 model.

The seasonal and regional model evaluations are conducted through soccer plots presented in Figs.5 and 6, summarizing the performance in both domains for the rural and urban sites, respectively. The observed and modeled surface rural PM_{10} levels over EU are compared in Fig.5a-d (upper panel). The results show a systematic underestimation for all models in almost all seasons and sub-regions. The largest underestimations for the rural PM_{10} are calculated for the EU3 sub-region (Mediterranean), particularly during winter (Fig.5a). In sub-region EU1, underestimations of 2% (in summer by SI1) to 74% (in winter by IT2) are calculated. In EU1, surface PM_{10} levels in autumn were overestimated by 1% and 4% by IT1 and SI1, respectively. In sub-region EU2, the highest underestimation (85%) was calculated for IT2 model again for the winter period (Fig.5a) while SI1 model had the smallest underestimations with values from 23% to 57%. UK4 model had the lowest underestimations for the spring and summer levels (Fig.5a,d) by 14% and 11%, respectively. Overall, the largest biases were calculated for the winter period (by up to 85%). Similar results were calculated for the urban surface PM_{10} levels in EU with slight lower biases (Fig.6a-d).

3.1.2. Seasonal vs regional surface levels over North America

Over NA, the temporal variation of rural PM_{10} levels is poorly reproduced by majority of the models with *PCC* of 0.22 to 0.38 (Table 2). CA2f model fails to reproduce the temporal variation (*PCC*=-0.05). The low values for this last model may be due to the lack of snow reduction factors in the reprocessing of emissions of fugitive dust for this model in this experiment (see Pouliot et al, 2014). On the other hand, the temporal variation at the urban sites are slightly better captured by the models (*PCC*=0.18-0.54). The *NMB* values do not differ much between the rural and urban stations on the continental scale (NA0) as seen in Table 2. Over both station types, ES1 and US8 models have the largest biases (>70%) while other models have much lower biases (<40%). The monthly variations in NA0 (NA0) are

296 better captured compared to the daily variability as seen in Figs.2 and 3. In sub-region NA1,
297 particularly over the rural stations, the majority of the models fail to reproduce both the
298 temporal variation and the magnitudes. In sub-regions NA2 and NA3, the temporal variability
299 is relatively better captured by the models. The variability in the observed PM_{10}
300 concentrations are relatively well represented by CA2f and US7 with low biases (< 20%) as
301 seen in Fig.4 (upper panel), but also by US6 with a larger bias over the rural (-39%) and urban
302 (-34%) stations (Table 2). Similar to the EU domain, the MACC model largely underpredicts
303 the observed variability.

304 The temporal variability of rural PM_{10} levels over the NA1 sub-region was poorly reproduced
305 by all models with *PCC* values ranging from 0.03 (CA2f) to 0.52 (US6). In NA2, PCC values
306 were also low; -0.16 (ES1) to 0.56 (US7). Temporal variations over NA3, however, were
307 reproduced reasonably well by most models (*PCC*=0.69 to 0.74) except for the ES1 model
308 (*PCC*=0.28). There is a general underestimation by all models in all sub-regions. As can be
309 seen in Fig.2, the largest underestimation occurs in NA1 (*MNB*=-57% to -84%) with the
310 exception of US7 overestimating by 19%. Over NA2 and NA3, underestimations from 20% to
311 88% are calculated. The largest underestimations are calculated for ES1 (*MNB*>80%) while
312 US7 had the smallest biases (<25%). Urban PM_{10} levels over NA are best reproduced in NA3
313 with *PCC* over 0.60 except for ES1 (*PCC*=0.33). PCC values range from 0.11 to 0.55 over
314 NA1 and from -0.15 to 0.72 over NA2. There are generally underestimations by up to 87% in
315 the sub-regions while CA2f and US7 overestimate the urban PM_{10} levels over NA1by 11%
316 and 20%, respectively. The largest biases are calculated for the ES1 model in all sub-regions
317 (*MNB*=80% to 87%).

318 Soccer plots for the seasonal and geographical model performance for the rural and urban
319 surface PM_{10} levels over NA are presented in Figs.5 and 6 (lower panels). Over NA, there are
320 no systematic seasonal trends in model performance except for the ES1 and US8 models
321 having the largest biases for rural PM_{10} levels in all seasons and sub-regions (Fig.5e-h). ES1
322 model follows US8 with slightly lower biases. The largest underestimations were calculated
323 for the spring and summer periods in all sub-regions by up to 90% and 93%, respectively.
324 There is a general underestimation in all seasons and sub-regions, with the exception of
325 overestimations calculated for US7 model by 3% to 67% over NA1. On a continental scale,
326 US7 model slightly overestimates the rural PM_{10} levels by 3%. The model performances for
327 the urban PM_{10} levels over NA (Fig.6e-h) are similar to those for the rural levels, with slightly
328 lower biases.

329 The large differences in PM_{10} predictions among those models and their performances at rural
330 and urban sites can be attributed mainly to the use of different online dust emission modules.
331 For example, US7 and US8 use two different dust emission modules available in WRF/Chem
332 version 3.4.1, i.e., the MOSAIC/GOCART dust module of Zhao et al. (2010) and
333 AER/AFWA dust module of Jones and Creighton (2011). The simulated coarse dust
334 concentrations by the two dust emission modules used by US7 and US8 are significantly
335 different in terms of locations and magnitudes (Fig.S1). While both simulate dust emissions
336 from the Mojave desert in southeastern California and the Sonoran Deserts in southern
337 Arizona, the MOSAIC/GOCART dust module gives much higher coarse dust emissions than

the AER/AFWA dust module in these areas with a much broader areal coverage and also predict dust emissions in many other areas in the continental U.S. and northern Mexico. As reported by Raman and Arellano (2013), the AER/AFWA dust emission module in WRF/Chem v. 3.4.1 significantly underpredicted dust emissions over Phoenix area in Arizona, U.S., resulting in significant underpredictions of PM_{10} (~50 mg m^{-3}) comparing to the observed concentration of 1800 □g m^{-3}. While differences in the dust emission modules explain most differences in coarse dust, another reason for much lower dust concentrations by US8 is the use of a simplified surface drag parameterization of Mass and Ovens (2010). While this parameterization helps reduce the overpredictions of wind speeds (Wang et al., 2014; Yahya et al., 2014a, b), it reduces dust emissions which depend strongly on wind speeds. The sensitivity simulation without the parameterization of Mass and Ovens (2010) gives dust concentrations that are higher by about a factor of two than the one with this parameterization. The substantial differences in coarse dust concentrations contribute to large differences in coarse PM between the two model simulations. Differences in sea-salt emissions predicted by US7 and US8 also contribute to differences in coarse PM concentrations, although their contributions to differences in PM_{10} performance at rural and urban locations are negligible (in particular, for sites located inland). Although US7 and US8 use the same sea-salt emission module of Gong et al. (1997), US8 gives lower sea-salt emissions (thus lower sea-salt concentrations) over oceanic areas because of the use of a simplified surface drag parameterization of Mass and Ovens (2010) that gives lower wind speeds.

3.2. $PM_{2.5}$

3.2.1. Seasonal and regional surface levels over Europe

All models show a very similar behavior for simulated continental surface rural and urban $PM_{2.5}$ levels compared to the simulated PM_{10} levels, with lower biases, as seen in the box-and-whisker plots presented in the lower panel of Fig.4. *PCC* values calculated for the simulated $PM_{2.5}$ levels are very similar in general to those calculated for the PM_{10} levels (Table 2). Over the rural stations, the underestimations range from 2% (CH1) to 60%, with the highest bias calculated for the IT2 model similar to PM_{10}. For the urban stations, the largest bias was again calculated for the IT2 model (*MNB*=68%). UK4 model overestimated the rural PM_{10} concentrations by 20% (Table 2) as can also be seen in Fig.7. The sub-regional analyses show that these overestimations are mostly due to the large overestimations particularly during summer in the Mediterranean region (EU3) by up to 72%. Further analyses have shown that these overestimates for UK4 are due to excessive model PM from wildfire emissions on the Iberian Peninsular where the vast majority of PM observations are located. The UK4 model has not previously been run for a domain with large sources of wildfires and it seems likely that the implementation of these sources needs further improvement in this model configuration. The MACC model underestimates the continental and annual mean levels as shown in Fig.4, as well as in all sub-regions and seasons, suggesting that these overestimations are not due to the boundary conditions, but may be due to the emissions or deposition. Dry deposition of $PM_{2.5}$ calculated by the models (Fig.9a) show that IT2 and SI1 models simulate significantly larger deposition compared to the other models. This can

explain the systematic largest underestimations associated with the IT2 model compared to the other models.

The soccer plots presented in Fig.10a and 11a show that winter levels are underestimated by all models in all sub-regions, in general by more than 50%, particularly over the urban stations. In other seasons, the underestimations are lower. CH1 and UK4 models overestimate in spring and in particular during summer. IT1 and SI1 overestimate rural EU3 $PM_{2.5}$ levels by 4% and 5%, respectively (Fig.10b). Similar overestimations hold for UK4 over the urban stations (Fig.11b). In summer, there is general underestimation by the majority of the models by up to 49% and 59% (by IT2 in EU2) over the rural and urban stations, respectively (Fig.10c and 11c). Autumn levels are underestimated by up to 72% over the rural (Fig.10d) and by up to 77% over the urban stations (Fig.11d) depending on the region with the maximum bias calculated for EU2 by the IT2 model.

3.2.2. Seasonal vs regional surface levels over North America

The temporal variations for the domain-averaged surface $PM_{2.5}$ concentrations over both rural and urban stations are much better captured by the majority of the models compared to the PM_{10} levels (Table 2). *PCC* values for the urban stations (0.31 to 0.78) are higher than those for the rural values (0.05 to 0.61) for all models, as can also be seen from the monthly time series plots in Fig.7 and 8. ES1 model had the lowest correlations while US7 had the highest values. ES1 model also had the largest biases (*MNB*=-68% and -71% for rural and urban stations, respectively) while US8 simulated the surface $PM_{2.5}$ levels with the lowest bias (*MNB*=-26% and -17%, respectively). The large underestimation calculated for the ES1 model can be attributed to the significantly larger dry deposition compare to the other models as can be seen in Fig.9b. As discussed in section 3.1.2, the underestimation in the PM_{10} levels for the US8 model suggests that the dust particles in both coarse and fine modes are significantly underestimated by this model. US7 model overestimated the domain-averaged $PM_{2.5}$ levels over both station types by ~48%, likely due to an overprediction in dust and sea-salt concentrations in $PM_{2.5}$ size sections. $PM_{2.5}$ concentrations predicted by US7 are much higher than those from US8 (Fig.S1). Such differences can be attributed to several factors. First, US7 and US8 use different dust emission modules, which give very different concentrations of dust in the $PM_{2.5}$ size sections/modes. Second, US7 and US8 use different splitting fractions between coarse and fine dust emissions. US7 allocates 9% and 68% of the total dust emission to $PM_{2.5}$ and coarse PM, respectively. Since MOSAIC only describes aerosols up to 10 μm, the emissions for particles with diameter greater than 10 μm are neglected (which is 23% of the total emissions). For comparison, US8 allocates 3% of dust emissions in the accumulation mode and the rest of 97% in the coarse mode. Third, US7 and US8 give different predictions of primary and secondary organic aerosols (POA and SOA), due possibly to the use of different SOA modules and different conversion factors between primary organic carbon emissions and the POA simulated in the model. As seen in Fig.4, the models have similar profiles for both rural and urban stations while the MACC model overestimates the rural and underestimates the urban $PM_{2.5}$ concentrations, implying that the simulated levels were due to local contributions rather than regional transport.

US7 model overestimates both the rural and urban $PM_{2.5}$ concentrations in all seasons and sub-regions (Fig.10 and 11e-h). The overestimations simulated by US7 model are smallest during winter from 16% to 96% over the rural and 51% to 82% over the urban stations. The figures also show that ES1 model underestimates in all seasons and sub-regions. With the exception of ES1 model, all models fall into the 75% error range in all seasons and sub-regions, while excluding US7, the error decreases to the 50% range (Fig.10 and 11e-h). Compared to the PM_{10} levels, the figures show that majority of the models are grouped around the zero line of the soccer plots. The differences in all seasons are highest in sub-region NA1over both rural (*MNB* up to 143%) and urban stations (*MNB* up to 95%).

3.2.3. $PM_{2.5}$ speciated components

Simulated surface sulfate (SO_4^{2-}), nitrate (NO_3^-) and ammonium (NH_4^+) components of $PM_{2.5}$ aerosols are compared with observations from five, six, and five rural stations in EU, respectively, and 250, 148 and 149 station in NA, respectively. The results are presented in Fig.12 in the soccer plots for the continental and sub-regional levels in 2010 over EU and NA. Over EU, the continental SO_4^{2-} levels are underestimated by a majority of the models (AT1, DE4, ES1, ES3, IT1, IT2 and UK5) by 22% to 61% (Fig.12a) while few groups (BG2, CH1, NL2, SI1 and UK4) overestimated the SO_4^{2-} levels by 7% to 52%. The results show that the underestimating models were all WRF/CHEM models, with the exception of SI1 that overestimates. The largest underestimation of SO_4^{2-} by IT2 can be attributed to the large SO_4^{2-} dry deposition calculated by this model (Fig.9a). SO_4^{2-} underestimation can also be attributed to absence of SO_2 oxidation in cloud water in the heterogeneous phase (e.g. the IT1 model: Balzarini et al., 2014). As seen in Fig.12b and c, simulated NO_3^- and NH_4 are higher than the observed levels. NO_3^- levels are overestimated by majority of the models in all regions by more than 75%, particularly in EU2 and EU3 (Fig.12b). NH_4^+ levels are also underestimated largely in EU3. In other sub-regions, the differences for simulated NH_4^+ levels are lower (50% to 75%). The results suggest ammonium nitrate (NH_4NO_3) formation dominating over the ammonium sulfate ($(NH_4)_2SO_4$) formation over EU as well as possible underestimations in heterogeneous (cloud) SO_4 formation and generation of fine sea-salt emissions.

The picture is completely opposite over the NA domain as seen in Fig.12d-f. SO_4^{2-} levels are particularly overestimated over NA1 as well as over the continent. Particularly CA2f model largely overestimates SO_4^{2-} levels in all sub-regions. NA2 and NA3 are characterized by underestimated SO_4^{2-} levels by the majority of the models. The differences from the observations are in general below 75% except for the CA2f model that has much larger bias. CA2f model has the smallest differences for both NO_3^- and NH_4^+ while ES1 model has the largest underestimations by more than a factor of 2.

3.3. Aerosol Optical Depth (AOD)

The reconstructed AOD at 555nm (AOD555) are compared with observations from 35 Aerosol Robotic Network (AERONET; http://aeronet.gsfc.nasa.gov/new_web/index.html) stations from each domain. Soccer plots and the diurnal profiles for the model performances in 2010 for the continental and sub-regional AOD555 levels are presented in Fig.13a,c. Over EU (Fig.12a), the majority of the model performed within the 50% error range. The DE3

model had the largest underestimations (*MNB*=60%) in all regions (Fig.13c) while the BG2 model had the largest overestimations (*MNB* up to 70%). The large underestimation by the DE3 model can be attributed to the approach in estimating the AOD555. While the majority of the models consider SO4, NO3, NH4, primary and secondary organic aerosols (POA/SOA), elemental carbon (EC), dust and sea-salt (Curci et al., 2014) in their AOD estimations, the DE3 model does not consider EC, POA/SOA and sea-salt. The smallest bias was calculated for SI1 (*MNB*=+7%) and for AT1 (-12%). In general, models BG2, CH1, NL2 and UK5 overestimated the observed AOD555 levels while other models underestimate. The observed hourly diurnal variation over the continent was moderately captured by the models with a maximum and minimum *PCC* of 0.65 (AT1) and 0.25 (DE3), respectively. WRF/CHEM models were associated with very similar temporal variations (*PCC*=~0.6). Over NA (Fig.13b,d), CA2f model failed to reproduce both the temporal variation (*PCC*=0.23) and the magnitude of the continental AOD555 with an overestimation of 29%. US6 model reproduced the temporal variation better than the other models (*PCC*=0.73), but with the largest bias (*MNB*=-32%). US7 also overestimated the continental AOD555 by 25% and captured the temporal variability (*PCC*=0.70) while US8 underestimated the observations by 17% with a temporal agreement of 0.65. Further discussion on model uncertainty on AOD calculation may be found in Curci et al. (2014).

4. Summary and Conclusions

An operational evaluation of simulated particulate matter (PM) levels over Europe (EU) and North America (NA) in 2010 using eight different on-line-coupled air quality models from sixteen groups has been conducted in the context of the AQMEII project. Seven groups from EU and two groups from NA applied the WRF/CHEM model, but with different settings. Anthropogenic emissions and chemical boundary conditions were prescribed while biogenic emissions were calculated online by each individual group. All groups interpolated their model output to a common output grid and a common set of receptor locations and uploaded the data to the ENSEMBLE system. The results are evaluated against surface and sounding observations, which are provided by operational over EU and NA, at continental and sub-regional levels on annual and seasonal basis.

Results show that over EU, particularly in winter, the monthly temporal variations were not captured by any of the models while the majority of the models produced spring and autumn peaks, particularly for the rural stations while these are not observed in the measurements or the MACC model, suggesting that the anthropogenic emissions or the online-simulated natural dust emissions can be responsible for these peaks. Over EU, the rural PM_{10} concentrations are underestimated by all models by up to 66% while the underestimations are much larger for the urban PM_{10} concentrations (up to 75%), suggesting that the urban emissions were not able to represent the actual emissions. The results show a systematic underestimation for all models in almost all seasons and sub-regions, with the largest underestimations for the Mediterranean region. The results also show overestimations in $PM_{2.5}$ levels suggesting the large underestimations in the PM_{10} levels can be attributed to the

503 natural emissions. Over NA, there are no systematic seasonal trends in model performances
504 except for the ES1 and US8 models having the largest biases for rural PM_{10} levels in all
505 seasons and sub-regions. There is a general underestimation in all seasons and sub-regions,
506 with the exception of overestimations calculated for US7 model by 3% to 67% over western
507 US. The highest underestimations were calculated for the spring and summer periods in all
508 sub-regions by up to ~90%. In general, majority of the models simulating the NA case have
509 smaller biases compared to those simulating the EU case, in particular regarding $PM_{2.5}$, which
510 suggests a better representation of the anthropogenic emissions in NA.

511 SO_4 levels over EU are underestimated by majority of the models by up to 61% while few
512 groups overestimated the SO_4 levels by 7% to 52%. NO_3 levels are overestimated by majority
513 of the models in all regions by more than 75%, particularly in east and south Europe while
514 NH_4 levels are also underestimated largely in south Europe. SO_4 levels over NA are
515 particularly overestimated over western US that is characterized by large anthropogenic
516 emissions. Eastern US is characterized by underestimated SO_4 levels by the majority of the
517 models. Regarding the AOD555, the majority of the model performed within the 50% error
518 range over EU. Differences in models can be attributed to differences in approaches in
519 estimating the AOD such as the aerosol components considered in these estimations. The
520 observed hourly diurnal variation over the continent was moderately captured by the models
521 while WRF/CHEM models were associated with very similar temporal variations. Over NA,
522 the CA2f and US7 models overestimate the observed AOD555 levels by up to 29% while the
523 US6 and US8 models underestimate by up to 32%. Results show that the simulated dry
524 deposition simulated can lead to substantial differences among the models.

525 Overall, the results show that representation of dust and sea-salt emissions can largely impact
526 the simulated PM concentrations and that there are still major challenges and uncertainties in
527 simulating the PM levels and identifying the source of the bias in the models. It should be
528 noted that as the results presented in this paper are temporally and spatially averaged over the
529 seasons and sub-regions, cases where feedback mechanisms are of importance must be further
530 studied and evaluated in order to better evaluate the skills of these models in simulating the
531 feedback mechanisms and their impact on the surface PM levels.

532

533 Acknowledgements

534 We gratefully acknowledge the contribution of various groups to the second air Quality
535 Model Evaluation international Initiative (AQMEII) activity: U.S. EPA, Environment Canada,
536 Mexican Secretariat of the Environment and Natural Resources (Secretaría de Medio
537 Ambiente y Recursos Naturales-SEMARNAT) and National Institute of Ecology (Instituto
538 Nacional de Ecología-INE) (North American national emissions inventories); U.S. EPA
539 (North American emissions processing); TNO (European emissions processing);
540 ECMWF/MACC project & Météo-France/CNRM-GAME (Chemical boundary conditions).
541 Ambient North American concentration measurements were extracted from Environment
542 Canada's National Atmospheric Chemistry Database (NAtChem) PM database and provided
543 by several U.S. and Canadian agencies (AQS, CAPMoN, CASTNet, IMPROVE, NAPS,

SEARCH and STN networks); North American precipitation-chemistry measurements were extracted from NAtChem's precipitation-chemistry data base and were provided by several U.S. and Canadian agencies (CAPMoN, NADP, NBPMN, NSPSN, and REPQ networks); the WMO World Ozone and Ultraviolet Data Centre (WOUDC) and its data-contributing agencies provided North American and European ozonesonde profiles; NASA's AErosol RObotic NETwork (AeroNet) and its data-contributing agencies provided North American and European AOD measurements; the MOZAIC Data Centre and its contributing airlines provided North American and European aircraft takeoff and landing vertical profiles; for European air quality data the following data centers were used: EMEP European Environment Agency/European Topic Center on Air and Climate Change/AirBase provided European air- and precipitation-chemistry data. The Finish Meteorological Institute is acknowledged for providing biomass burning emission data for Europe. Data from meteorological station monitoring networks were provided by NOAA and Environment Canada (for the US and Canadian meteorological network data) and the National Center for Atmospheric Research (NCAR) data support section. Joint Research Center Ispra/Institute for Environment and Sustainability provided its ENSEMBLE system for model output harmonization and analyses and evaluation. The co-ordination and support of the European contribution through COST Action ES1004 EuMetChem is gratefully acknowledged. The views expressed here are those of the authors and do not necessarily reflect the views and policies of the U.S. Environmental Protection Agency (EPA) or any other organization participating in the AQMEII project. This paper has been subjected to EPA review and approved for publication. C. Knote was supported by the DOE grant DE-SC0006711. The UPM authors thankfully acknowledge the computer resources, technical expertise and assistance provided by the Centro de Supercomputación y Visualización de Madrid (CESVIMA) and the Spanish Supercomputing Network (BSC). G. Curci and P. Tuccella were supported by the Italian Space Agency (ASI) in the frame of PRIMES project (contract n.I/017/11/0). The Centre of Excellence for Space Sciences and Technologies SPACE-SI is an operation partly financed by the European Union, European Regional Development Fund and Republic of Slovenia, Ministry of Higher Education, Science, Sport and Culture. Y. Zhang acknowledges funding support from the NSF Earth System Program (AGS-1049200) and high-performance computing support from Yellowstone by NCAR’s Computational and Information Systems Laboratory, sponsored by the National Science Foundation and Stampede, provided as an Extreme Science and Engineering Discovery Environment (XSEDE) digital service by the Texas Advanced Computing Center (TACC). The technical assistance of Bert van Ulft (KNMI) and Arjo Segers (TNO) in producing the results of the RACMO2-LOTOS-EUROS system is gratefully acknowledged. L. Giordano was supported by the Swiss SERI COST project C11.0144. UH-CAIR acknowledges support from the TRANSPHORM (FP7) project which provided the basis for their modelling approaches.

REFERENCES

585 Ahmadov, R., McKeen, S. A., Robinson, A., Bahreini, R., Middlebrook, A., de Gouw, J.,
586 Meagher, J., Hsie, E., Edgerton, E., Shaw, S., Trainer, M., 2012. A volatility basis set model
587 for summertime secondary organic aerosols over the eastern United States in 2006. Journal of
588 Geophysical Research, 117, D06301.
589
590 Ackermann, I.J., Hass, H., Memmesheimer, M., Ebel, A., Binkowski, F.S., Shankar, U., 1998.
591 Modal aerosol dynamics model for Europe: Development and first applications. Atmospheric
592 Environment, 32, 17, 2981-2999.
593
594 Appel, K. W., Pouliot, G. A., Simon, H., Sarwar, G., Pye, H. O. T., Napelenok, S. L., Akhtar,
595 F., Roselle, S. J., 2013. Evaluation of dust and trace metal estimates from the Community
596 Multiscale Air Quality (CMAQ) model version 5.0. Geoscientific Model Development, 6,
597 883-899.
598
599 Appel, K.W., Bhave, P.V., Gilliland, A.B., Sarwar, G., Roselle, S.J., 2008. Evaluation of the
600 community multiscale air quality (CMAQ) model version 4.5: Sensitivities impacting model
601 performance; Part II particulate matter. Atmospheric Environment, 42, 6057– 6066.
602
603 Baklanov, A., Schlünzen, K., Suppan, P., Baldasano, J., Brunner, D., Aksoyoglu, S.,
604 Carmichael, G., Douros, J., Flemming, J., Forkel, R., Galmarini, S., Gauss, M., Grell, G.,
605 Hirtl, M., Joffre, S., Jorba, O., Kaas, E., Kaasik, M., Kallos, G., Kong, X., Korsholm, U.,
606 Kurganskiy, A., Kushta, J., Lohmann, U., Mahura, A., Manders-Groot, A., Maurizi, A.,
607 Moussiopoulos, N., Rao, S. T., Savage, N., Seigneur, C., Sokhi, R. S., Solazzo, E.,
608 Solomos, S., Sørensen, B., Tsegas, G., Vignati, E., Vogel, B., Zhang, Y., 2014. Online
609 coupled regional meteorology chemistry models in Europe: current status and prospects.
610 Atmospheric Chemistry and Physics, 14, 317-398.
611
612 Balzarini, A., Pirovano, G., Honzak, L., Zabkar, R., Curci, G., Forkel, R., Hirtl, M., San José,
613 R., Tuccella, P., Grell, G.A., 2014. WRF-Chem model sensitivity to chemical mechanism
614 choice in reconstructing aerosol optical properties. Atmospheric Environment, Submitted.
615
616 Bellouin, N., Rae, J., Jones, A., Johnson, C., Haywood, J., Boucher, O., 2011. Aerosol forcing
617 in the Climate Model Intercomparison Project (CMIP5) simulations by HadGEM2-ES and the
618 role of ammonium nitrate. Journal of Geophysical Research-Atmosphere, 116, D20206.
619
620 Beltman, J.B., Hendriks, C., Tum, M., Schaap, M., 2013. The impact of large scale biomass
621 production on ozone air pollution in Europe. Atmospheric Environment, 71, 352-363.
622
623 Bernard, S.M., Samet, J.M., Grambsch, A., Ebi, K.L., Romieu, I., 2001. The potential
624 impact of climate variability and change on air pollution-related health effects in
625 the United States. Environmental Health Perspectives 109 (Suppl. 2), 199-209.
626
627 Bianconi, R., Galmarini, S., Bellasio, R., 2004.Web-based system for decision support
628 in case of emergency: ensemble modelling of long-range atmospheric dispersion
629 of radionuclides. Environmental Modelling and Software 19, 401-411.
630
631 Brunner, D., Jorba, O., Savage, N., Eder, B., Makar, P., Giordano, L., Badia, A., Balzarini, A.,
632 Baro, R., Bianconi, R., Chemel, C., Forkel, R., Jimenez-Guerrero, P., Hirtl, M., Hodzic, A.,
633 Honzak, L., Im, U., Knote, C., Kuenen, J.J.P., Makar, P.A., Manders-Groot, A., Neal, L.,
634 Perez, J.L., Pirovano, G., San Jose, R., Savage, N., Schroder, W., Sokhi, R.S., Syrakov, D.,

Torian, A., Werhahn, K., Wolke, R., van Meijgaard, E., Yahya, K., Zabkar, R., Zhang, Y., Zhang, J., Hogrefe, C., Galmarini, S., 2014. Evaluation of the meteorological performance of coupled chemistry-meteorology models in phase 2 of the Air Quality Model Evaluation International Initiative. Atmospheric Environment, to be submitted.

Curci, G., Balzarini, A., Baró, R., Bianconi, R., Brunner, D., Forkel, R., Giordano, L., Hirtl, M., Hogrefe, C., Honzak, L., Im, U., Jiménez-Guerrero, P., Knote, C., Langer, M., Makar, P., Pirovano, G., Pérez, J.L., San José, R., Syrakov, D., Tuccella, P., Werhahn, J., Wolke, R., Žabkar, R., 2014. Uncertainties of simulated aerosol optical properties induced by assumptions on aerosol physical and chemical properties, Atmospheric Environment, Submitted.

Fountoukis, C., Nenes, A., 2007. ISORROPIA II: a computationally efficient thermodynamic equilibrium model for K^+–Ca^{2+}–Mg^{2+}–NH^{4+}–Na^+–SO_4^{2-}–NO_3^-–Cl^-–H_2O aerosols. Atmospheric Chemistry and Physics, 7, 4639-4659.

Galmarini, S., Rao, S.T., 2011. The AQMEII two-continent Regional Air Quality Model evaluation study: Fueling ideas with unprecedented data. Atmospheric Environment, 45, 2464.

Galmarini, S., Bianconi, R., Appel, W., Solazzo, E., et al., 2012. ENSEMBLE and AMET: two systems and approaches to a harmonised, simplified and efficient assistance to air quality model developments and evaluation. Atmospheric Environment, 53, 51-59.

Gong, S.L., Barrie, L.A., Blanchet, J.-P., von Salzen, K., Lohmann, U., Lesins, G., Spacek, L., Zhang, L.M., Girard, E., Lin, H., Leaitch, R., Leighton, H., Chylek, P., Huang, P., 2003b. Canadian Aerosol Module: A size-segregated simulation of atmospheric aerosol processes for climate and air quality models 1. Module development. Journal of Geophysical Research: Atmospheres, 108, D01, AAC 3-1 – AAC 3-16.

Gong, S.L., 2003. A parameterization of sea-salt aerosol source function for sub- and super-micron particles. Global Biogeochemical Cycles 17 (4), 1097.

Gong, S.L., Barrie, L.A., Blanchet, J.-P., 1997. Modeling sea-salt aerosols in the atmosphere 1. Model development. Journal of Geophysical Research, 102 (D3), 3805-3818.

Grell, G.A. Baklanov, A., 2011. Integrated modelling for forecasting weather and air quality: a call for fully coupled approaches. Atmospheric Environment, 45, 6845–6851.

Grell, G.A., Peckham, S.E., Schmitz, R., McKeen, S.A., Frost, G., Skamarock, W.C., Eder, B., 2005. Fully coupled "online" chemistry within the WRF model. Atmospheric Environment, 39, 6957-6975.

Guenther, A., Karl, T., Harley, P., Wiedinmyer, C., Palmer, P.I., Geron, C., 2006. Estimates of global terrestrial isoprene emissions using MEGAN (Model of Emissions of Gases and Aerosols from Nature. Atmospheric Chemistry and Physics, 6, 3181-3210.

Guenther, A.B., Zimmerman, P.R., Harley, P.C., Monson, R.K., Fall, R., 1993. Isoprene and monoterpene rate variability: model evaluations and sensitivity analyses. Journal of Geophysical Research, 98, D7, 12609-12617.

Hogrefe, C., Roselle, S., Mathur, R., Rao, S.T., Galmarini, S., 2014. Space-time analysis of the Air Quality Model Evaluation International Initiative (AQMEII) Phase 1 air quality simulations. Journal of Air Waste Management Association, 64, 388-405.

Im, U., Bianconi, R., Solazzo, E., Kioutsioukis, I., Badia, A., Balzarini, A., Baro, R., Bellasio, R., Brunner, D., Chemel, C., Curci, G., Flemming, J., Forkel, R., Giordano, L., Jimenez-Guerrero, P., Hirtl, M., Hodzic, A., Honzak, L., Jorba, O., Knote, C., Kuenen, J.J.P., Makar, P.A., Manders-Groot, A., Neal, L., Perez, J.L., Pirovano, G., Pouliot, G., San Jose, R., Savage, N., Schroder, W., Sokhi, R.S., Syrakov, D., Torian, A., Tuccella, P., Werhahn, K., Wolke, R., Yahya, K., Zabkar, R., Zhang, Y., Zhang, J., Hogrefe, C., Galmarini, S., 2014. Evaluation of operational online-coupled regional air quality models over Europe and North America in the context of AQMEII phase 2. Part I: Ozone. Atmospheric Environment, Submitted.

Inness, A., Baier, F., Benedetti, A., Bouarar, I., Chabrillat, S., Clark, H., Clerbaux, C., Coheur, P., Engelen, R. J., Errera, Q., Flemming, J., George, M., Granier, C., Hadji-Lazaro, J., Huijnen, V., Hurtmans, D., Jones, L., Kaiser, J. W., Kapsomenakis, J., Lefever, K., Leitão, J., Razinger, M., Richter, A., Schultz, M. G., Simmons, A. J., Suttie, M., Stein, O., Thépaut, J.-N., Thouret, V., Vrekoussis, M., Zerefos, C., and the MACC team, 2013. The MACC reanalysis: an 8 yr data set of atmospheric composition. Atmospheric Chemistry and Physics, 13, 4073-4109.

IPCC: Climate change, 2007. Synthesis Report, Intergovernmental Panel on Climate Change.

Jacob, D.J., Winner, D.A., 2009. Effect of climate change on air quality. Atmospheric Environment 41, 51-63.

Jones, S., Creighton, G.., 2011. AFWA dust emission scheme for WRF/Chem-GOCART. 2011 WRF workshop, June 20-24, Boulder, CO, USA.

Kelly, J.T., Bhave, P.V., Nolte, C.G., Shankar, U., Foley, K.M., 2010. Simulating emissions and chemical evolution of coarse sea-salt particles in the Community Multiscale Air Quality (CMAQ) model. Geoscientific Model Development 3, 257-273.

Kioutsioukis, I., Im, U., Bianconi, R., Badia, A., Balzarini, A., Baró, R., Bellasio, R., Brunner, D., Chemel, C., Curci, G., Denier van der Gon, H., Flemming, J., Forkel, R., Giordano, L., Jiménez-Guerrero, P., Hirtl, M., Jorba, O., Manders-Groot, A., Neal, L., Pérez, J.L., Piravano, G., San Jose, R., Savage, N., Schroder, W., Sokhi, R.S., Solazzo, E., Syrakov, D., Tuccella, P., Werhahn, J., Wolke, R., Hogrefe, C., Galmarini, S., 2014. Challenges in the deterministic skill of air quality ensembles. Atmospheric Environment, Submitted.

Kuenen, J.J.P., Visschedijk, A.J.H., Jozwicka, M., Denier van der Gon, H.A.C., 2014. TNO_MACC_II emission inventory: a multi-year (2003-2009) consistent high-resolution European emission inventory for air quality modelling. Atmospheric Chemistry and Physics Discussions, 14, 5837-5869.

Kulmala, M., Asmi, A., Lappalainen, H. K., Baltensperger, U., Brenguier, J.-L., Facchini, M. C., Hansson, H.-C., Hov, Ø., O'Dowd, C. D., Pöschl, U., Wiedensohler, A., Boers, R.,

Boucher, O., de Leeuw, G., Denier van der Gon, H. A. C., Feichter, J., Krejci, R., Laj, P., Lihavainen, H., Lohmann, U., McFiggans, G., Mentel, T., Pilinis, C., Riipinen, I., Schulz, M., Stohl, A., Swietlicki, E., Vignati, E., Alves, C., Amann, M., Ammann, M., Arabas, S., Artaxo, P., Baars, H., Beddows, D. C. S., Bergström, R., Beukes, J. P., Bilde, M., Burkhart, J. F., Canonaco, F., Clegg, S. L., Coe, H., Crumeyrolle, S., D'Anna, B., Decesari, S., Gilardoni, S., Fischer, M., Fjaeraa, A. M., Fountoukis, C., George, C., Gomes, L., Halloran, P., Hamburger, T., Harrison, R. M., Herrmann, H., Hoffmann, T., Hoose, C., Hu, M., Hyvärinen, A., Hõrrak, U., Iinuma, Y., Iversen, T., Josipovic, M., Kanakidou, M., Kiendler-Scharr, A., Kirkevåg, A., Kiss, G., Klimont, Z., Kolmonen, P., Komppula, M., Kristjánsson, J.-E., Laakso, L., Laaksonen, A., Labonnote, L., Lanz, V. A., Lehtinen, K. E. J., Rizzo, L. V., Makkonen, R., Manninen, H. E., McMeeking, G., Merikanto, J., Minikin, A., Mirme, S., Morgan, W. T., Nemitz, E., O'Donnell, D., Panwar, T. S., Pawlowska, H., Petzold, A., Pienaar, J. J., Pio, C., Plass-Duelmer, C., Prévôt, A. S. H., Pryor, S., Reddington, C. L., Roberts, G., Rosenfeld, D., Schwarz, J., Seland, Ø., Sellegri, K., Shen, X. J., Shiraiwa, M., Siebert, H., Sierau, B., Simpson, D., Sun, J. Y., Topping, D., Tunved, P., Vaattovaara, P., Vakkari, V., Veefkind, J. P., Visschedijk, A., Vuollekoski, H., Vuolo, R., Wehner, B., Wildt, J., Woodward, S., Worsnop, D. R., van Zadelhoff, G.-J., Zardini, A. A., Zhang, K., van Zyl, P. G., Kerminen, V.-M., S Carslaw, K., Pandis, S. N., 2011. General overview: European Integrated project on Aerosol Cloud Climate and Air Quality interactions (EUCAARI) – integrating aerosol research from nano to global scales. Atmospheric Chemistry and Physics, 11, 13061-13143.

Long M.S., Keene W.D., Kieber D.J., Erickson D.J., Maring H., 2011. A sea-state based source function for size- and composition-resolved marine aerosol production. Atmospheric Chemistry and Physics, 11, 1203-1216.

Lundgren, K., 2006. Numerical simulation of the spatial and temporal distribution of sea salt particles on the regional scale. M. Sc. thesis, Department of Meteorology Stockholm University, Stockholm, Sweden, 2006.

Makar, P.A., Gong, W., Hogrefe, C., Zhang, Y., Curci, G., Zabkar, R., Milbrandt, J., Im, U., Galmarini, S., Balzarini A., Baro, R., Bianconi, R., Cheung, P., Forkel, R., Gravel, S., Hirtl, M., Honzak, L., Hou, A., Jimenez-Guerrero, P., Langer M., Moran, M.D., Pabla, B., Perez, P.L., Pirovano, G., San Jose, R., Tuccella, P., Werhahn, J., Zhang, J., 2014a. Feedbacks between Air Pollution and Weather, Part 1: Effects on Chemistry. Atmospheric Environment, Submitted.

Makar, P.A., Gong, W., Hogrefe, C., Zhang, Y., Curci, G., Zabkar, R., Milbrandt, J., Im, U., Galmarini, S., Balzarini A., Baro, R., Bianconi, R., Cheung, P., Forkel, R., Gravel, S., Hirtl, M., Honzak, L., Hou, A., Jimenez-Guerrero, P., Langer M., Moran, M.D., Pabla, B., Perez, P.L., Pirovano, G., San Jose, R., Tuccella, P., Werhahn, J., Zhang, J., 2014b. Feedbacks between Air Pollution and Weather, Part 2: Effects on Weather. Atmospheric Environment, Submitted.

Mansell, G.E., Lau, S., Russel, J., Omary. M., 2006. Final report: Fugitive wind blown dust emissions and model performance evaluation: Phase II. Report prepared for Western Governors Association. Novato, Cal.: Environ International Corp.

Pouliot, G., Denier van der Gon, H., Kuenen, J., Makar, P., Zhang, J., Moran, M., 2014. Analysis of the Emission Inventories and Model-Ready Emission Datasets of Europe and North America for Phase 2 of the AQMEII Project. Atmospheric Environment, Submitted.

Raman, A., Arellano, A., 2013. Modeling and Data Analysis of 2011 Phoenix Dust Storm. oral presentation at the 15th Conference on Atmospheric Chemistry/93rd AMS annual meeting, Austin, Texas, U.S.A., 6-10 January.

Riemer, N., Vogel, H., Vogel, B., Fiedler, F., 2003. Modeling aerosols on the mesoscale-γ: Treatment of soot aerosol and its radiative effects. Journal of Geophysical Research, 108: doi: 10.1029/2003JD003448. issn: 0148-0227.

Savage, N. H., Agnew, P., Davis, L. S., Ordóñez, C., Thorpe, R., Johnson, C. E., O'Connor, F. M., Dalvi, M., 2013. Air quality modelling using the Met Office Unified Model (AQUM OS24-26): model description and initial evaluation. Geoscientific Model Development, 6, 353-372.

Schaap, M., Manders, A. M. M., Hendriks, E. C. J., Cnossen, J. M., Segers, A. J. S., Denier van der Gon, H. A. C., Jozwicka, M., Sauter, F., Velders, G., Matthijsen, J., Builtjes, P. J. H., 2009. Regional modelling of particulate matter for the Netherlands. PBL Report 500099008, Netherlands Environmental Assessment Agency, AH Bilthoven, the Netherlands, 2009.

Schaap, M., M. Roemer, F. Sauter, G. Boersen, R. Timmermans, P.J.H. Builtjes, 2005. LOTOS-EUROS: Documentation, TNO report B&O-A, 2005-297, Apeldoorn, 2005.

Shaw, W.J., Allwine, K.J., Fritz, B.G., Rutz, F.C., Rishel, J.P., Chapman, E.G., 2008. An evaluation of the wind erosion module in DUSTRAN. Atmospheric Environment, 42, 1907-1921.

Schell B., Ackermann, I. J., Hass, H., Binkowski, F.S., Ebel, A., 2001. Modeling the formation of secondary organic aerosol within a comprehensive air quality model system. Journal of Geophysical Research, 106, 28275-28293.

Schere, K., Flemming, J., Vautard, R., Chemel, C., Colette, A., Hogrefe, C., Bessagnet, B., Meleux, F., Mathur, R., Roselle, S., Hu, R.-M., Sokhi, R. S., Rao, S.T., S. Galmarini, 2012: Trace gas/aerosol boundary concentrations and their impacts on continental-scale AQMEII modeling domains, Atmospheric Environment, 53, 38-50.

Schwartz, J., Dockery, D.W., Neas, L.M., 1996. Is daily mortality associated specifically with fine particles? Journal of Air and Waste Management Association 46, 927-939.

Schwede, D., Pouliot, G., Pierce, T., 2005. Changes to the Biogenic Emissions Inventory System version 3 (BEIS3). In: 4th CMAS Models-3 Users' Conference, Chapel Hill, NC, 26–28 September 2005.

Soares, J., Sofiev, M., Prank, M, San Jose, R., Perez, J.L., 2014. On uncertainties of wild-land fires emission in AQMEII case study. Atmospheric Environment, In preparation.

Sofiev, M., Vankevich, R., Lotjonen, M., Prank, M., Petukhov, V., Ermakova, T., Koskinen, J., Kukkonen, J., 2009. An operational system for the assimilation of the satellite information on wild-land fires for the needs of air quality modelling and forecasting. Atmospheric Chemistry and Physics, 9, 6833-6847.

Solazzo, E., Bianconi, R., Pirovano, G., Moran, M., Vautard, R., Hogrefe, C., Appel, K.W., Matthias, V., Grossi, P., Bessagnet, B., Brandt, J., Chemel, C., Christensen, J.H., Forkel, R., Francis, X.V., Hansen, A., McKeen, S., Nopmongcol, U., Prank, M., Sartelet, K.N., Segers, A., Silver, J.D., Yarwood, G., Werhahn, J., Zhang, J., Rao, S.T., Galmarini, S. 2013. Evaluating the capabilities of regional scale air quality models to capture the vertical distribution of pollutants. Geoscientific Model Development 6, 791-818, 2013.

Solazzo, E., Bianconi, R., Vautard, R., Appel, K. W., Moran, M. D., Hogrefe, C., Bessagnet, B., 5 Brandt, J., Christensen, J. H., Chemel, C., Coll, I., van der Gon, H. D., Ferreira, J., Forkel, R., Francis, X. V., Grell, G., Grossi, P., Hansen, A. B., Jericevic, A., Kraljevic, L., Miranda, A. I., Nopmongcol, U., Pirovano, G., Prank, M., Riccio, A., Sartelet, K. N., Schaap, M., Silver, J. D., Sokhi, R. S., Vira, J., Werhahn, J., Wolke, R., Yarwood, G., Zhang, J., Rao, S. T., Galmarini, S., 2012a. Ensemble modelling of surface level ozone in Europe and North America in the context of AQMEI. Atmospheric Environment, 53, 60–74.

Solazzo, E., Bianconi, R., Pirovano, G., Matthias, V., Vautard, R., Moran, M. D., Appel, K. W., Bessagnet, B., Brandt, J., Christensen, J. H., Chemel, C., Coll, I., Ferreira, J., Forkel, R., Francis, X. V., Grell, G., Grossi, P., Hansen, A. B., Hogrefe, C., Miranda, A. I., Nopmongco, U., Prank, M., Sartelet, K. N., Schaap, M., Silver, J. D., Sokhi, R. S., Vira, J., Werhahn, J., Wolke, R., Yarwood, G., Zhang, J., Rao, S. T., Galmarini, S., 2012b. Operational model evaluation for particulate matter in Europe and North America in the context of AQMEII. Atmospheric Environment, 53, 75–92.

Tegen, I., Harrison, S.P., Kohfeld, K.E., Prentice, I.C., Coe, M.C., Heimann, M., 2002. The impact of vegetation and preferential source areas on global dust aerosol: results from a model study. Journal of Geophysical Research 107, doi:10.1029/2001JD000963

Vautard, R., Moran, M. D., Solazzo, E., Gilliam, R. C., Matthias, V., Bianconi, R., Chemel, C., Ferreira, J., Geyer, B., Hansen, A. B., Jericevic, A., Prank, M., Segers, A., Silver, J. D., Werhahn, J., Wolke, R., Rao, S. T., and Galmarini, S.: Evaluation of the meteorological forcing used for AQMEII air quality simulations, Atmos. Environ., 53, 15–37, 2012.

Vogel, B., Vogel, H., Baumer, D., Bangert, M., Lundgren, K., Rinke, R., Stanelle, T., 2009. The comprehensive model system COSMO-ART – Radiative impact of aerosol on the state of the atmosphere on the regional scale. Atmospheric Chemistry and Physics, 9, 8661–8680.

Wang, K., Yahya, K., Zhang, Y., Wu, S.-Y., Grell, G., 2014. Implementation and Initial Application of A New Chemistry-Aerosol Option in WRF/Chem for Simulation of Secondary Organic Aerosols and Aerosol Indirect Effects. Atmospheric Environment, in review.

Winker, D.M., Tackett, J.L., Getzewich, B.J., Liu, Z., Vaughan, V.A., Rogers, R.R., 2013. The global 3-D distribution of tropospheric aerosols as characterized by CALIOP. Atmospheric Chemistry and Physics, 13, 3345-3361.

Wolke, R., Schroder, W., Schrodner, R., Renner, E., 2012. Influence of grid resolution and meteorological forcing on simulated European air quality: a sensitivity study with the modeling system COSMO–MUSCAT. Atmospheric Environment 53, 110–130.

884 Wong, D. C., Pleim, J., Mathur, R., Binkowski, F., Otte, T., Gilliam, R., Pouliot, G., Xiu, A.,
885 Young, J. O., Kang, D., 2012. WRF-CMAQ two-way coupled system with aerosol feedback:
886 software development and preliminary results. Geoscientific Model Development, 5, 299-312.
887
888 Yahya, K., Wang, K., Zhang, Y., Kleindienst, T. E., 2014a. Application of WRF/Chem over
889 North America under the AQMEII Phase II. Part II. Comprehensive Evaluation of 2010
890 Simulation and Responses of Air Quality and Meteorology-Chemistry Interactions to Changes
891 in Emissions and Meteorology from 2006 to 2010. Atmospheric Environment, in preparation.
892
893 Yahya, K., Wang, K., Gudoshava, M., Glotfelty, T., Zhang, Y., 2014b. Application of
894 WRF/Chem over North America under the AQMEII Phase II. Part I. Comprehensive
895 Evaluation of 2006 Simulation. Atmospheric Environment, in review.
896
897 Zaveri, R.A., Easter, R.C., Fast, J.D., Peters, L.K., 2008. Model for simulating aerosol
898 interactions and chemistry (MOSAIC). Journal of Geophysical Research, 113, D13204.
899
900 Zhang, Y., 2008. Online-coupled meteorology and chemistry models: history, current status,
901 and outlook. Atmospheric Chemistry and Physics, 8, 2895–2932.
902
903 Zhao, C., Liu, X., Leung, L. R., Johnson, B., McFarlane, S. A., Gustafson Jr., W. I., Fast, J.
904 D., Easter, R., 2010. The spatial distribution of mineral dust and its shortwave radiative
905 forcing over North Africa: modeling sensitivities to dust emissions and aerosol size
906 treatments. Atmospheric Chemistry and Physics, 10, 8821-8838.

Table

Click here to download Table: Im_etal_PMcollective_Tables.docx

Table 1. Model groups participated to AQMEII2

No	Acronym	Domain	Model	Resolution	Biogenic Model	Dust Model	Sea-salt Model	Aerosol	Reference
1	AT1	EU	WRF/Chem	23 km	MEGAN[1]	MOSAIC[3] MADE[4]/SORGAM[5]	MOSAIC MADE/SORGAM	MADE/SORGAM	Grell et al., 2005
2	BG2	EU	WRF-CMAQ	25 km	BEIS[2]	Mansell et al., 2006	AERO4[9]	AERO4	Appel et al., 2008
3	CH1	EU	COSMO-ART	0.22 °	Gunter et al., 1998	Vogel et al., 2006	Lundgren, 2006	MADEsoot[10]	Vogel et al., 2009
4	DE3	EU	COSMO-MUSCAT	0.25 °	Gunther et al., 1993	Tegen et al., 2002	Long et al., 2011	Simpson et al., 2003	Wolke et al., 2012
5	DE4	EU	WRF/Chem	23 km	MEGAN	MOSAIC MADE/SORGAM	MOSAIC MADE/SORGAM	MADE/SORGAM	Grell et al., 2005
6	ES1	EU	WRF/Chem	23 km	MEGAN	MOSAIC MADE/SORGAM	MOSAIC MADE/SORGAM	MADE/SORGAM	Grell et al., 2005
7	ES3	EU	WRF/Chem	23 km	MEGAN	*N/A*	MOSAIC MADE/SORGAM	MOSAIC 4 bins	Grell et al., 2005
8	IT1	EU	WRF/Chem	23 km	MEGAN	MOSAIC MADE/SORGAM	MOSAIC MADE/SORGAM	MADE/SORGAM	Grell et al., 2005
9	IT2	EU	WRF/Chem	23 km	MEGAN	DUSTRUN[6]	MOSAIC MADE/SORGAM	MADE/VBS[11]	Grell et al., 2005
10	NL2	EU	RACMO LOTOS-EUROS	0.5°×0.25°	Beltman et al., 2013	Schaap et al., 2009	Schaap et al., 2009	ISORRAPIA II 2 bins [12]	Sauter et al., 2012
11	SI1	EU	WRF/Chem	23 km	MEGAN	MOSIC MADE/SORGAM	MOSAIC MADE/SORGAM	MADE	Grell et al., 2005
12	UK4	EU	MetUM UKCA- RAQ	0.22 °	TNO	Woodward, 2001	*N/A*	Bellouin et al., 2011	Savage et al., 2013
13	UK5	EU	WRF-CMAQ	18 km	MEGAN	*N/A*	Kelly et al., 2010	AERO6[14]	Wong et al., 2012
14	CA2f	NA	GEM-MACH	15 km	BEIS	*N/A*	Gong et al., 2003	CAM[13]	Makar et al., 2014a,b
15	ES1	NA	WRF/Chem	36 km	MEGAN	MOSAIC MADE/SORGAM	MOSAIC MADE/SORGAM	MADE/SORGAM	Grell et al., 2005
16	US6	NA	WRF-CMAQ	12 km	BEIS3.14	Appel et al., 2013	Kelly et al., 2010	AERO6	Wong et al., 2012
17	US7	NA	WRF/Chem	36 km	MEGAN	GOCART AFWA[7]	Gong et al., 1997	MOSAIC	Grell et al., 2005
18	US8	NA	WRF/Chem	36 km	MEGAN	AFWA/AER[8]	Gong et al., 1997	MADE/VBS	Grell et al., 2005

1. Guenther et al., 2006; 2. Schwede et al., 2005; 3. Zaveri et al., 2008; 4. Ackermann et al., 1998; 5. Schell et al., 2001; 6. Schaw et al., 2008; 7. Jones and Creighton, 2011; 8. XXX; 9. Appel et al., 2008; 10. Riemer et al., 2003; 11. Ahmadov et al., 2012; 12. Fountoukis and Nenes, 2007; 13. Gong et al., 2003b.14. Appel et al., 2013

Table 2. Statistical comparisons of observed and simulated annual and domain-mean surface PM_{10} and $PM_{2.5}$ over EU and NA

Models	PM_{10}								$PM_{2.5}$							
	Rural				Urban				Rural				Urban			
	r	*NMSE* (%)	*NMB* (%)	*RMSE* ($\mu g\ m^{-3}$)	*r*	*NMSE* (%)	*NMB* (%)	*RMSE* ($\mu g\ m^{-3}$)	*r*	*NMSE* (%)	*NMB* (%)	*RMSE* ($\mu g\ m^{-3}$)	*r*	*NMSE* (%)	*NMB* (%)	*RMSE* ($\mu g\ m^{-3}$)
AT1	0.40	55.34	-43.55	11.06	0.34	125.19	-61.70	22.72	0.34	38.17	-31.67	6.91	0.38	72.32	-45.33	11.14
BG2	0.74	55.30	-46.86	10.72	0.76	141.76	-65.14	23.07	0.80	33.27	-36.58	6.22	0.84	62.53	-47.46	10.15
CH1	0.42	29.93	-28.52	9.17	0.27	85.20	-53.82	20.64	0.29	24.42	-1.28	6.67	0.34	34.71	-24.58	9.10
DE3	0.63	45.54	-41.88	10.18	0.58	130.79	-63.26	22.75	0.60	23.70	-24.82	5.71	0.67	49.99	-40.07	9.70
DE4	0.18	59.13	-43.64	11.42	0.06	125.63	-61.30	22.88	0.11	44.01	-31.74	7.42	0.08	82.12	-46.42	11.75
ES1	0.22	74.83	-49.19	12.20	0.16	152.22	-65.15	23.90	0.21	52.93	-38.19	7.74	0.22	94.45	-50.72	12.09
ES3	0.35	77.96	-50.74	12.26	0.11	182.13	-68.38	24.90	0.23	44.98	-34.03	7.37	0.28	81.27	-47.52	11.57
IT1	0.57	21.70	-25.12	7.97	0.47	68.83	-50.29	19.20	0.52	16.70	-12.28	5.18	0.56	35.91	-29.89	8.89
IT2	0.26	168.83	-66.10	14.97	0.25	270.45	-75.24	26.86	0.16	132.25	-59.65	9.89	0.23	209.61	-67.99	14.51
NL2	0.61	34.54	-35.68	9.32	0.57	97.69	-57.61	21.12	0.65	41.25	-37.94	6.85	0.75	81.28	-50.94	11.19
SI1	0.62	17.63	-21.52	7.36	0.57	62.11	-48.67	18.53	0.60	13.84	-9.33	4.80	0.60	30.67	-27.30	8.37
UK4	0.25	31.91	-23.29	9.79	0.07	53.46	-42.58	18.18	0.03	55.49	19.42	11.02	0.16	28.54	-8.34	9.06
UK5	0.86	50.34	-46.32	10.28	0.82	116.40	-61.83	21.88	0.84	48.04	-44.39	7.00	0.90	81.46	-53.39	10.92
EU Mean	0.64	43.49	-40.29	10.08	0.52	109.88	-59.55	21.88	0.49	28.54	-26.70	6.19	0.60	57.47	-41.61	10.26
EU Median	0.68	50.52	-43.50	10.57	0.56	124.21	-61.95	22.56	0.56	34.57	-32.37	6.55	0.64	68.40	-45.85	10.78
CA2f	-0.10	49.37	-19.79	15.64	0.33	5.40	-4.72	5.68	0.51	10.23	19.67	2.47	0.65	11.15	29.42	3.99
ES1	0.41	344.08	-76.91	22.15	0.16	363.46	-81.04	20.81	0.05	175.80	-67.97	5.29	0.24	250.59	-74.98	8.32
US6	0.21	63.65	-38.22	15.58	0.34	19.85	-31.43	9.25	0.41	11.07	-6.05	2.27	0.68	7.90	8.58	3.08
US7	0.20	34.17	-17.21	13.22	0.55	7.79	-18.06	6.33	0.61	20.84	46.89	3.90	0.56	16.15	36.11	4.93
US8	0.31	438.30	-80.09	23.22	0.49	216.12	-73.74	18.88	0.46	18.99	-25.49	2.65	0.62	13.81	-24.87	3.39
NA Mean	0.24	83.01	-46.45	16.57	0.60	33.85	-42.10	11.10	0.58	7.31	-6.78	1.84	0.74	3.54	-5.30	1.92
NA Median	0.18	115.82	-54.21	18.10	0.54	46.72	-47.43	12.42	0.55	9.19	-11.69	2.01	0.72	4.07	-6.48	2.05

Figure Captions

Fig.1. Standard annual $PM_{2.5}$ emissions in Europe and North America overlaid with monitoring stations in the sub-regions (upper panel: the red circles show EU1/NA1, yellow diamonds show EU2/NA2 and green squares show EU3/NA3) and monthly time series of anthropogenic $PM_{2.5}$ emissions over EU and NA (lower panel). Note scale differences.

Fig.2. Observed and simulated monthly continental and sub-regional rural PM_{10} concentrations over EU (upper panel) and NA (lower panel). Note scale differences.

Fig.3. Observed and simulated monthly continental and sub-regional urban PM_{10} concentrations over EU (upper panel) and NA (lower panel). Note scale differences.

Fig.4. Box-and-whisker plots for observed and simulated PM_{10} (upper panel) and $PM_{2.5}$ (lower panel) concentrations over rural and urban stations in Europe and North America.

Fig.5. Soccer plots for simulated seasonal and regional rural PM_{10} levels over Europe (upper panel) and North America (lower panel) for winter (a,e), spring (b,f), summer (c,g) and autumn (d,h).

Fig.6. Soccer plots for simulated seasonal and regional urban PM_{10} levels over Europe (upper panel) and North America (lower panel) for winter (a,e), spring (b,f), summer (c,g) and autumn (d,h).

Fig.7. Observed and simulated monthly continental and sub-regional rural $PM_{2.5}$ concentrations over EU (upper panel) and NA (lower panel). Note scale differences.

Fig.8. Observed and simulated monthly continental and sub-regional urban $PM_{2.5}$ concentrations over EU (upper panel) and NA (lower panel). Note scale differences.

Fig.9. Calculated annual dry deposition of fine inorganic aerosols (SO_4, NO_3 and NH_4), total organic carbon (TOC) $PM_{2.5}$, crustal material (CM) and sea-salt (SS) over a,b) EU and c,d) NA.

Fig.10. Soccer plots for simulated seasonal and regional rural $PM_{2.5}$ levels over Europe (upper panel) and North America (lower panel) for winter (a,e), spring (b,f), summer (c,g) and autumn (d,h).

Fig.11. Soccer plots for simulated seasonal and regional urban $PM_{2.5}$ levels over Europe (upper panel) and North America (lower panel) for winter (a,e), spring (b,f), summer (c,g) and autumn (d,h).

Fig.12. Soccer plots for simulated regional rural fine SO_4 (a,d), NO_3 (b,e) and NH_4 (c,f) levels over Europe (upper panel) and North America (lower panel).

Fig.13. Soccer (a,b) and diurnal time series (c,d) plots for observed and simulated AOD555 over Europe (a,c) and North America (b,d).

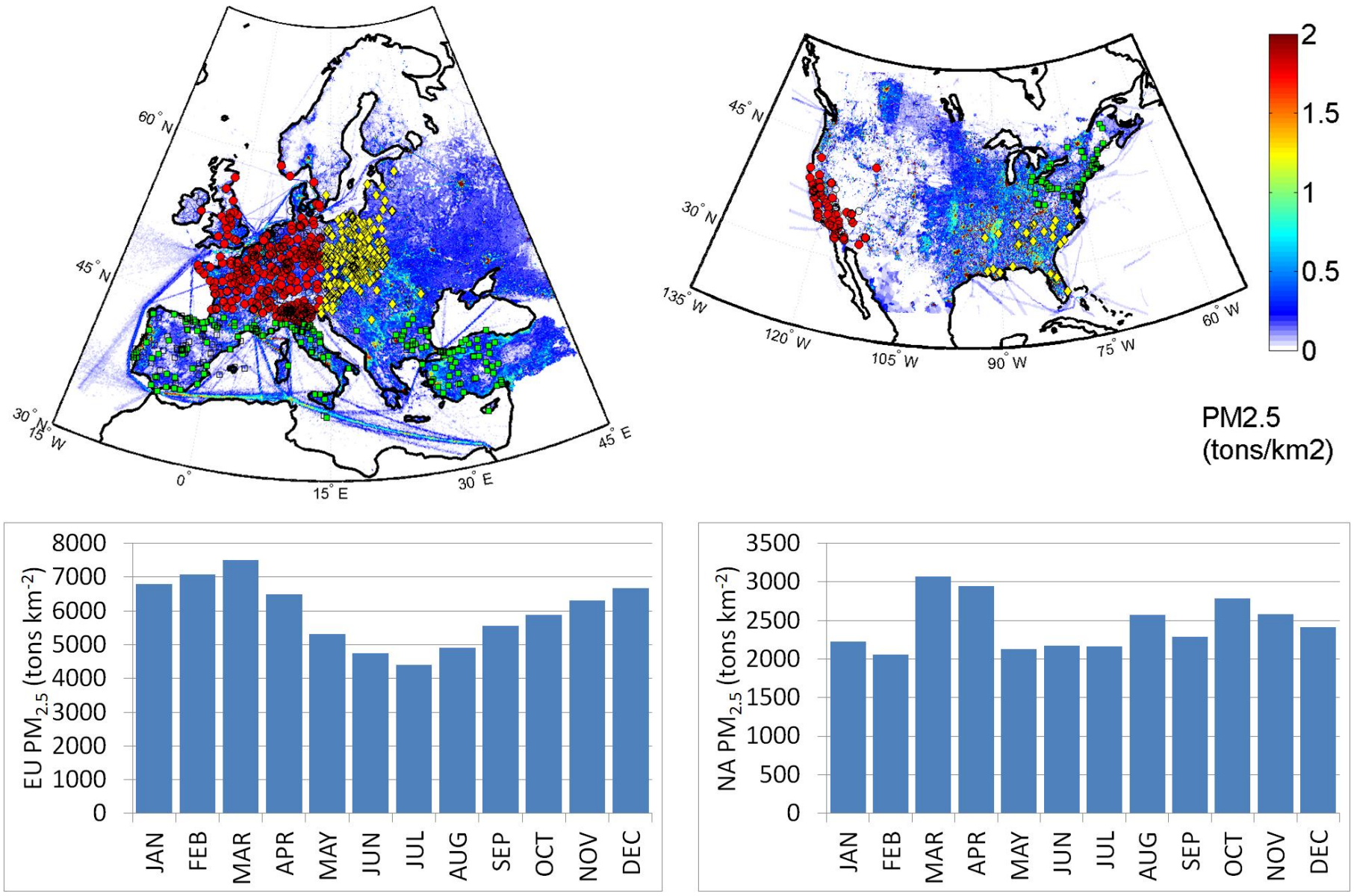
60° N
45° N
30° N
15° W
0°
15° E
30° E
45° E
45° N
30° N
135° W
120° W
105° W
90° W
75° W
60° W
2
1.5
1
0.5
0
PM2.5
(tons/km2)
EU PM2.5 (tons km-2)
8000
7000
6000
5000
4000
3000
2000
1000
0
JAN
FEB
MAR
APR
MAY
JUN
JUL
AUG
SEP
OCT
NOV
DEC
NA PM2.5 (tons km-2)
3500
3000
2500
2000
1500
1000
500
0
JAN
FEB
MAR
APR
MAY
JUN
JUL
AUG
SEP
OCT
NOV
DEC

Fig.1

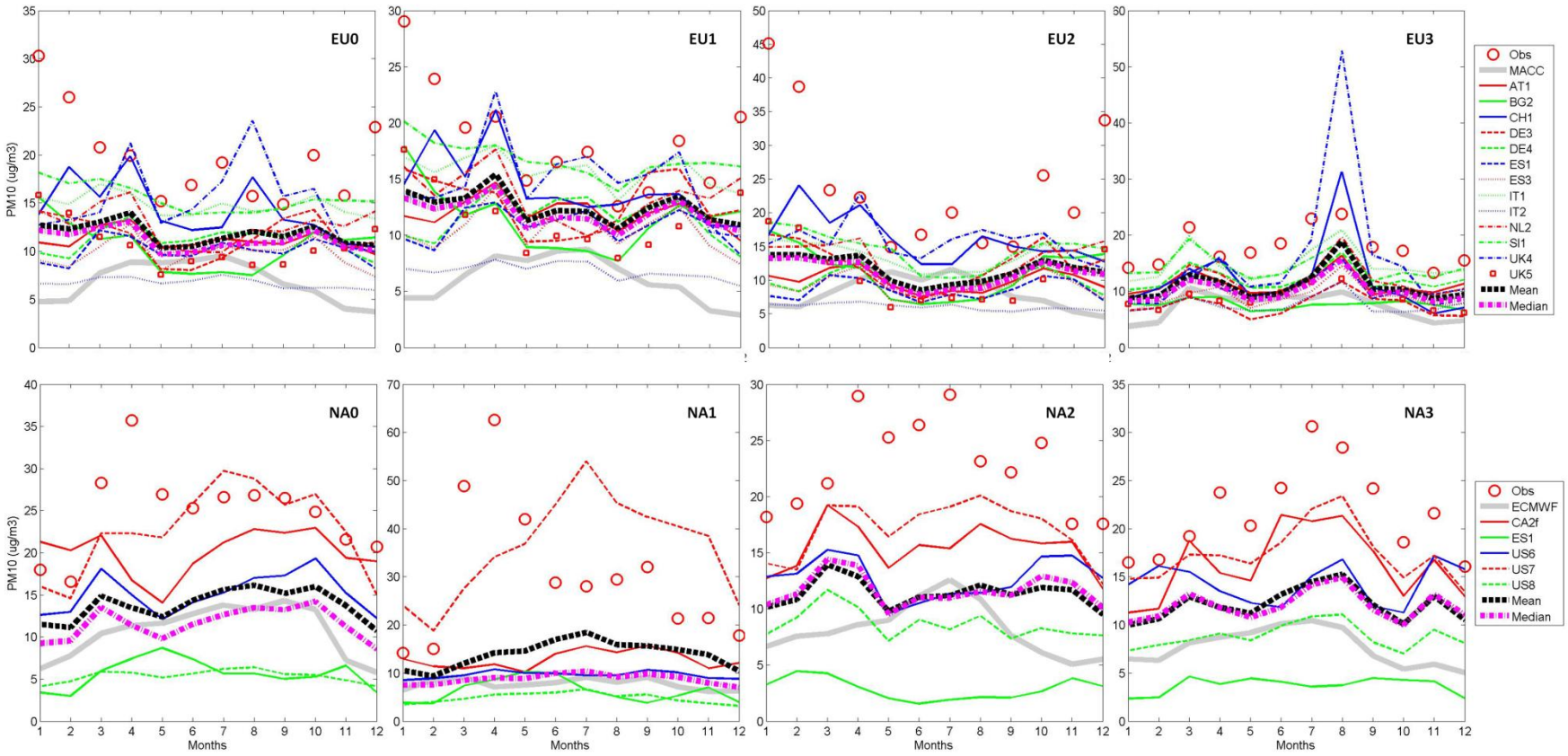
EU0
EU1
EU2
EU3
NA0
NA1
NA2
NA3
PM10 (ug/m3)
Months
Obs
MACC
AT1
BG2
CH1
DE3
DE4
ES1
ES3
IT1
IT2
NL2
SI1
UK4
UK5
Mean
Median
Obs
ECMWF
CA2f
ES1
US6
US7
US8
Mean
Median

Fig.2

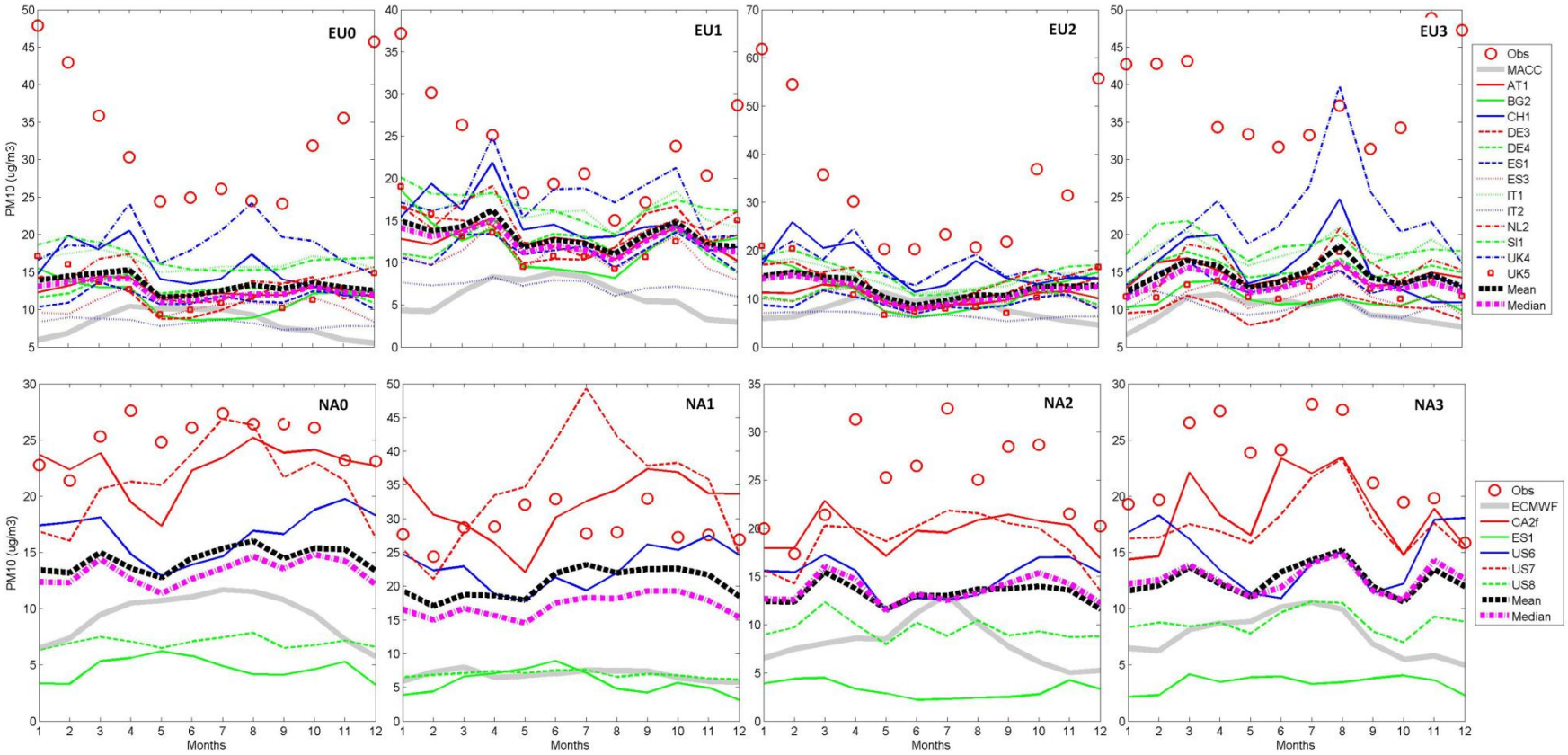
EU0
EU1
EU2
EU3
NA0
NA1
NA2
NA3
PM10 (ug/m3)
Months
Obs
MACC
AT1
BG2
CH1
DE3
DE4
ES1
ES3
IT1
IT2
NL2
SI1
UK4
UK5
Mean
Median
Obs
ECMWF
CA2f
ES1
US6
US7
US8
Mean
Median

Fig.3

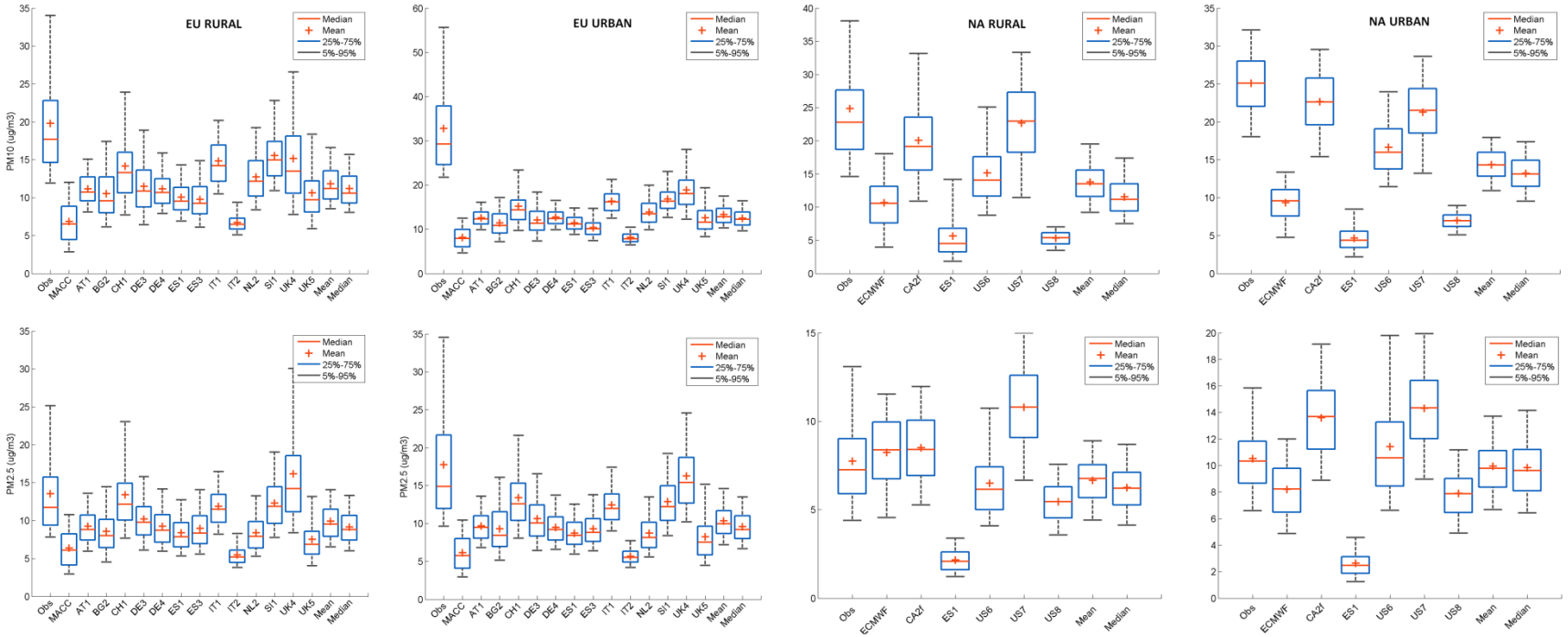
EU RURAL
EU URBAN
NA RURAL
NA URBAN
PM10 (ug/m3)
PM2.5 (ug/m3)
Median
Mean
25%-75%
5%-95%
Obs
MACC
AT1
BG2
CH1
DE3
DE4
ES1
ES3
IT1
IT2
NL2
SI1
UK4
UK5
Mean
Median
ECMWF
CA2f
US6
US7
US8

Fig.4

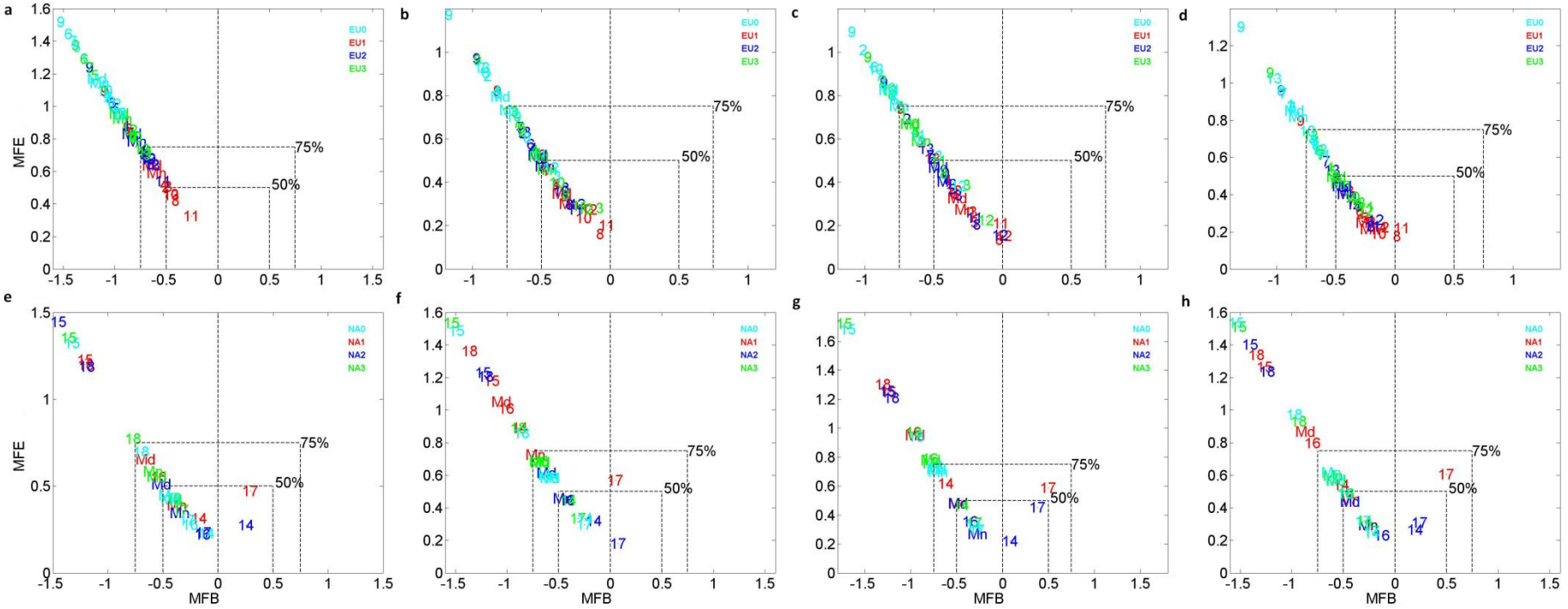

Fig.5

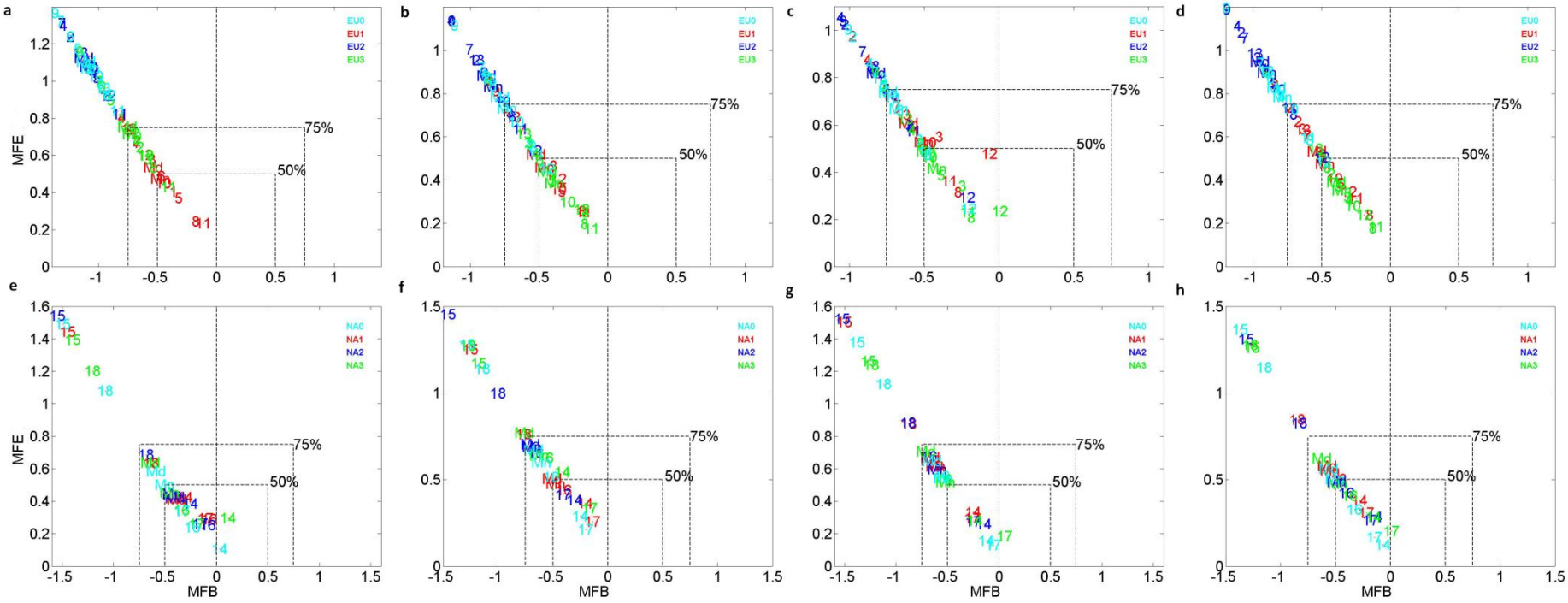

Fig.6

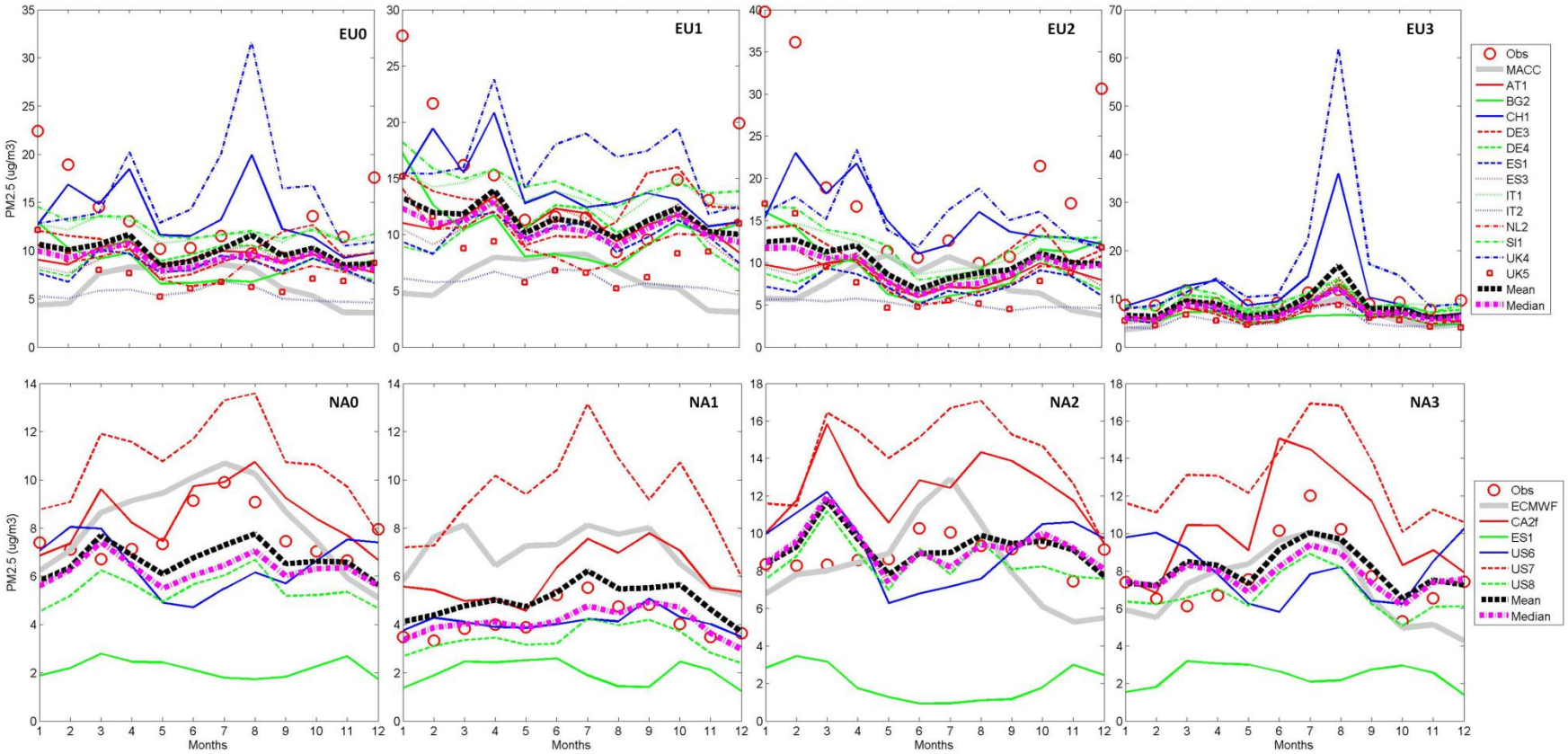
EU0
EU1
EU2
EU3
NA0
NA1
NA2
NA3
PM2.5 (ug/m3)
Months
Obs
MACC
AT1
BG2
CH1
DE3
DE4
ES1
ES3
IT1
IT2
NL2
SI1
UK4
UK5
Mean
Median
Obs
ECMWF
CA2f
ES1
US6
US7
US8
Mean
Median

Fig.7

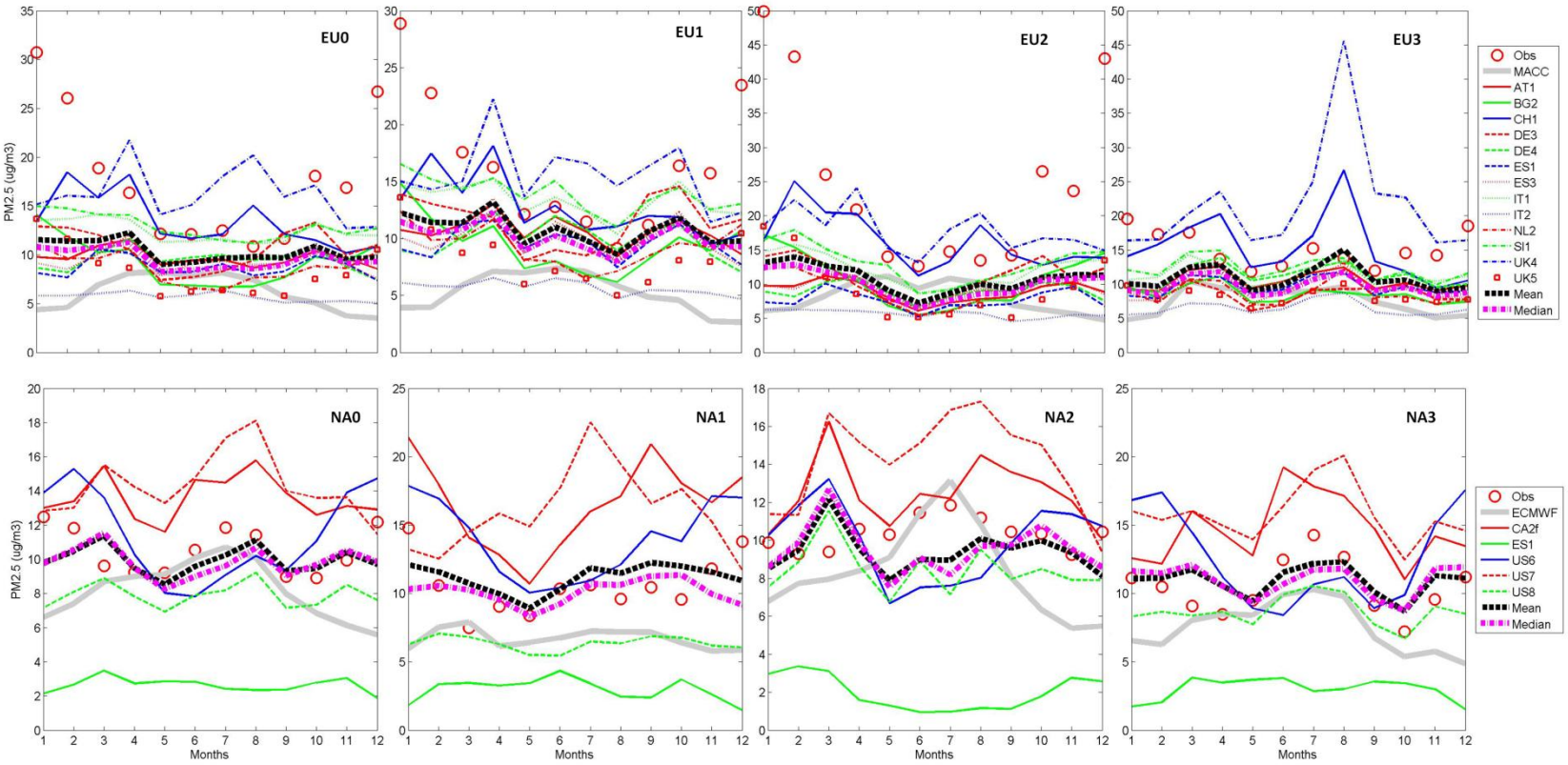
EU0
EU1
EU2
EU3
NA0
NA1
NA2
NA3
PM2.5 (ug/m3)
Months
Obs
MACC
AT1
BG2
CH1
DE3
DE4
ES1
ES3
IT1
IT2
NL2
SI1
UK4
UK5
Mean
Median
Obs
ECMWF
CA2f
ES1
US6
US7
US8
Mean
Median

Fig.8

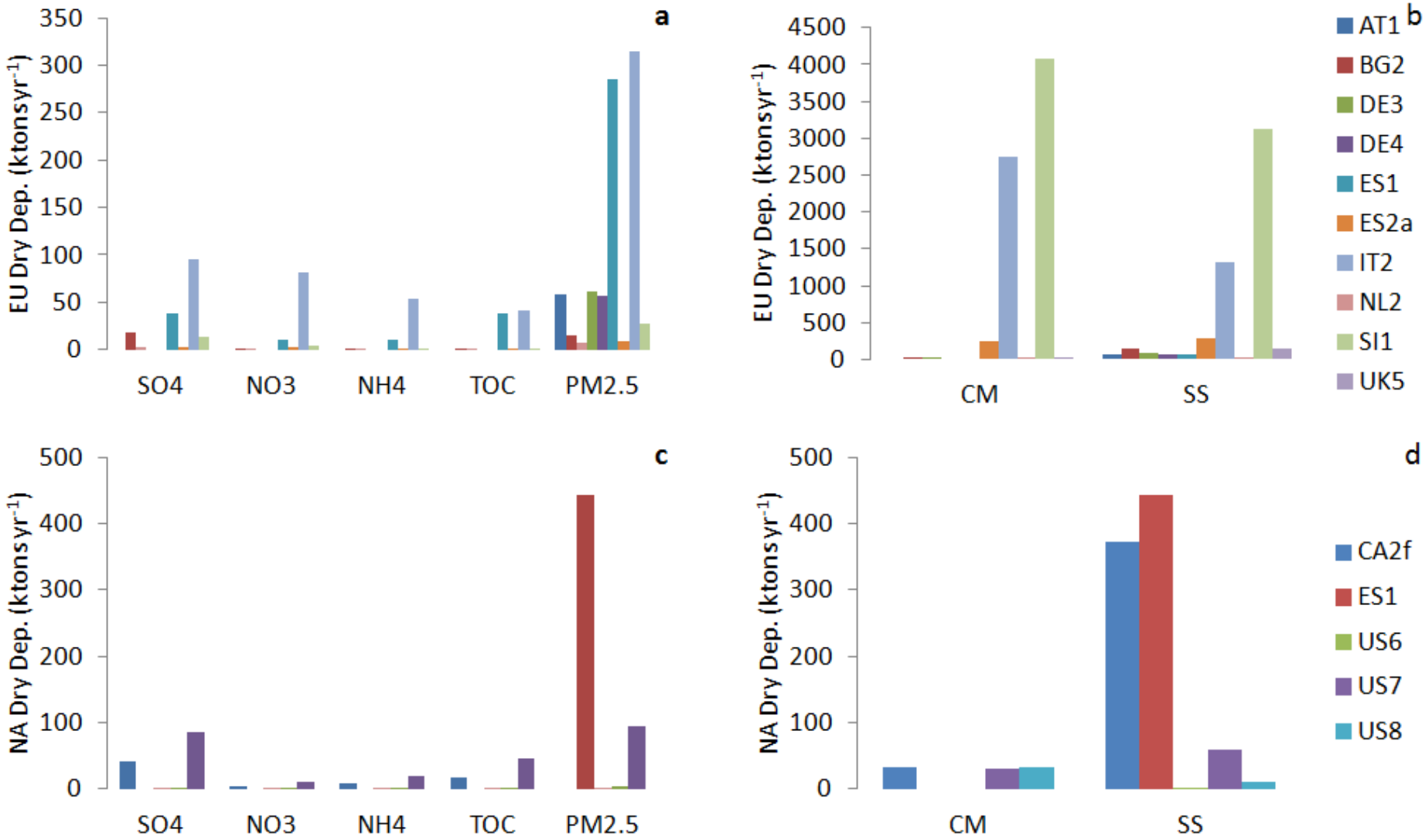
a
EU Dry Dep. (ktonsyr-1)
350
300
250
200
150
100
50
0
SO4
NO3
NH4
TOC
PM2.5
b
EU Dry Dep. (ktonsyr-1)
4500
4000
3500
3000
2500
2000
1500
1000
500
0
CM
SS
AT1
BG2
DE3
DE4
ES1
ES2a
IT2
NL2
SI1
UK5
c
NA Dry Dep. (ktonsyr-1)
500
400
300
200
100
0
SO4
NO3
NH4
TOC
PM2.5
d
NA Dry Dep. (ktonsyr-1)
500
400
300
200
100
0
CM
SS
CA2f
ES1
US6
US7
US8

Fig.9

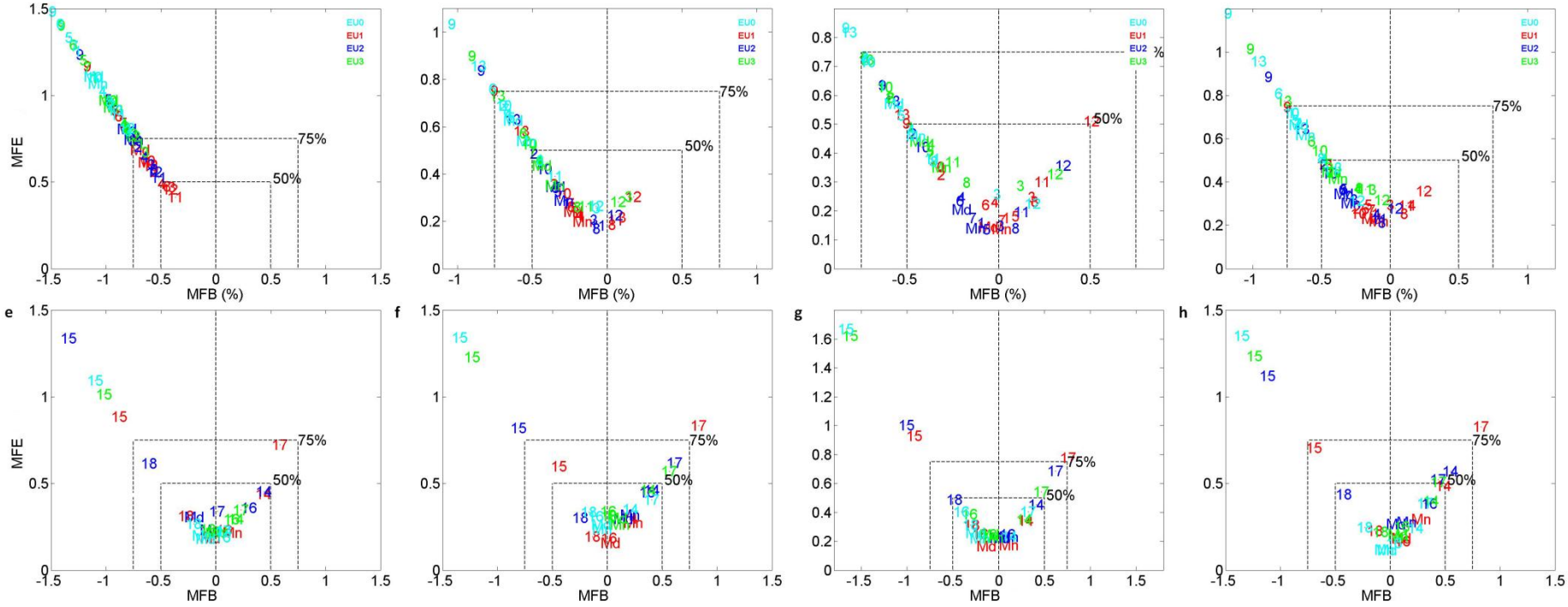

Fig.10

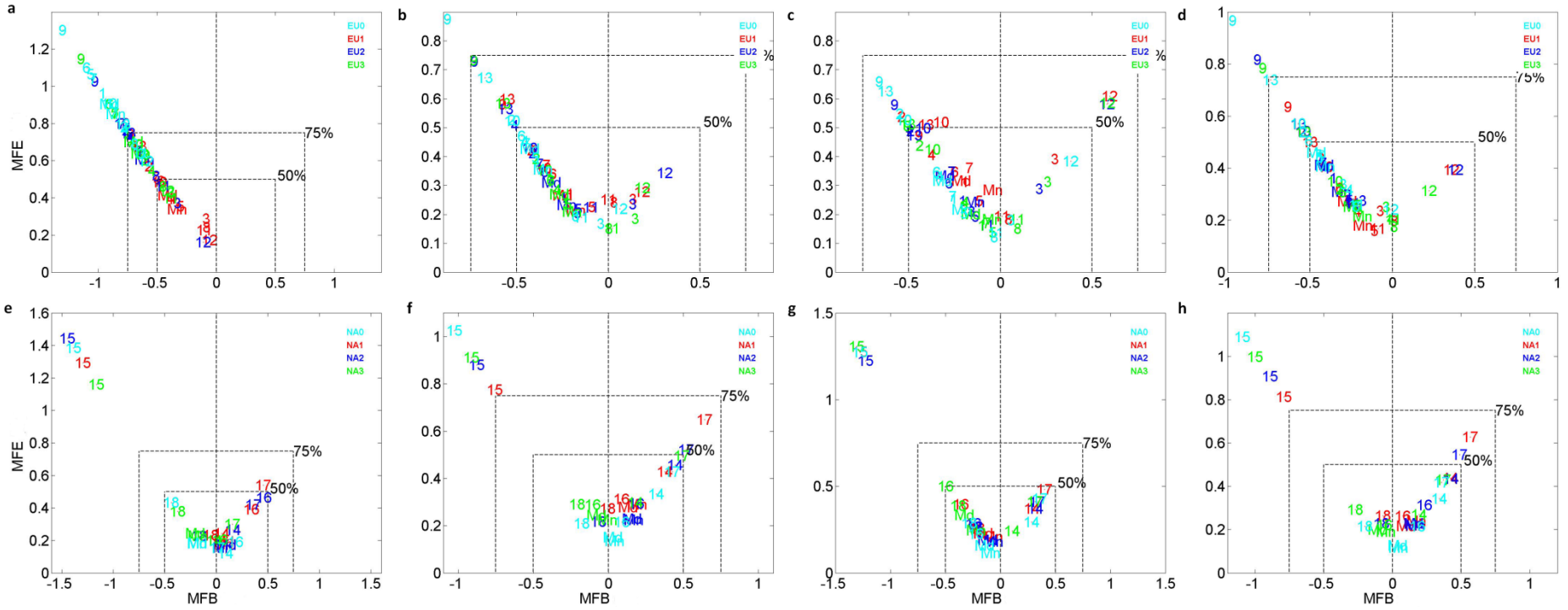

Fig.11

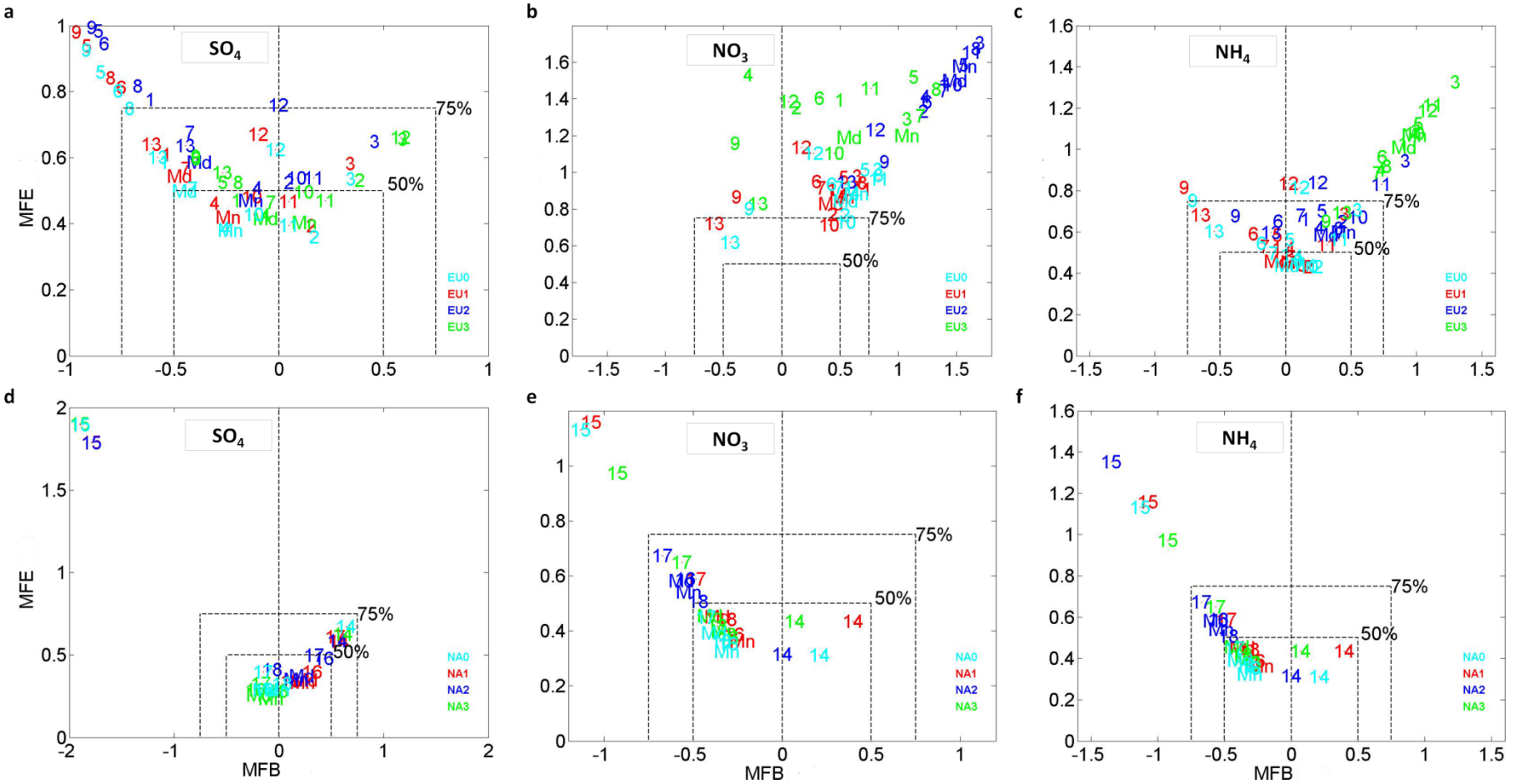
a
SO4
MFE
75%
50%
EU0
EU1
EU2
EU3
b
NO3
75%
50%
EU0
EU1
EU2
EU3
c
NH4
75%
50%
EU0
EU1
EU2
EU3
d
SO4
MFE
MFB
75%
50%
NA0
NA1
NA2
NA3
e
NO3
MFB
75%
50%
NA0
NA1
NA2
NA3
f
NH4
MFB
75%
50%
NA0
NA1
NA2
NA3

Fig.12

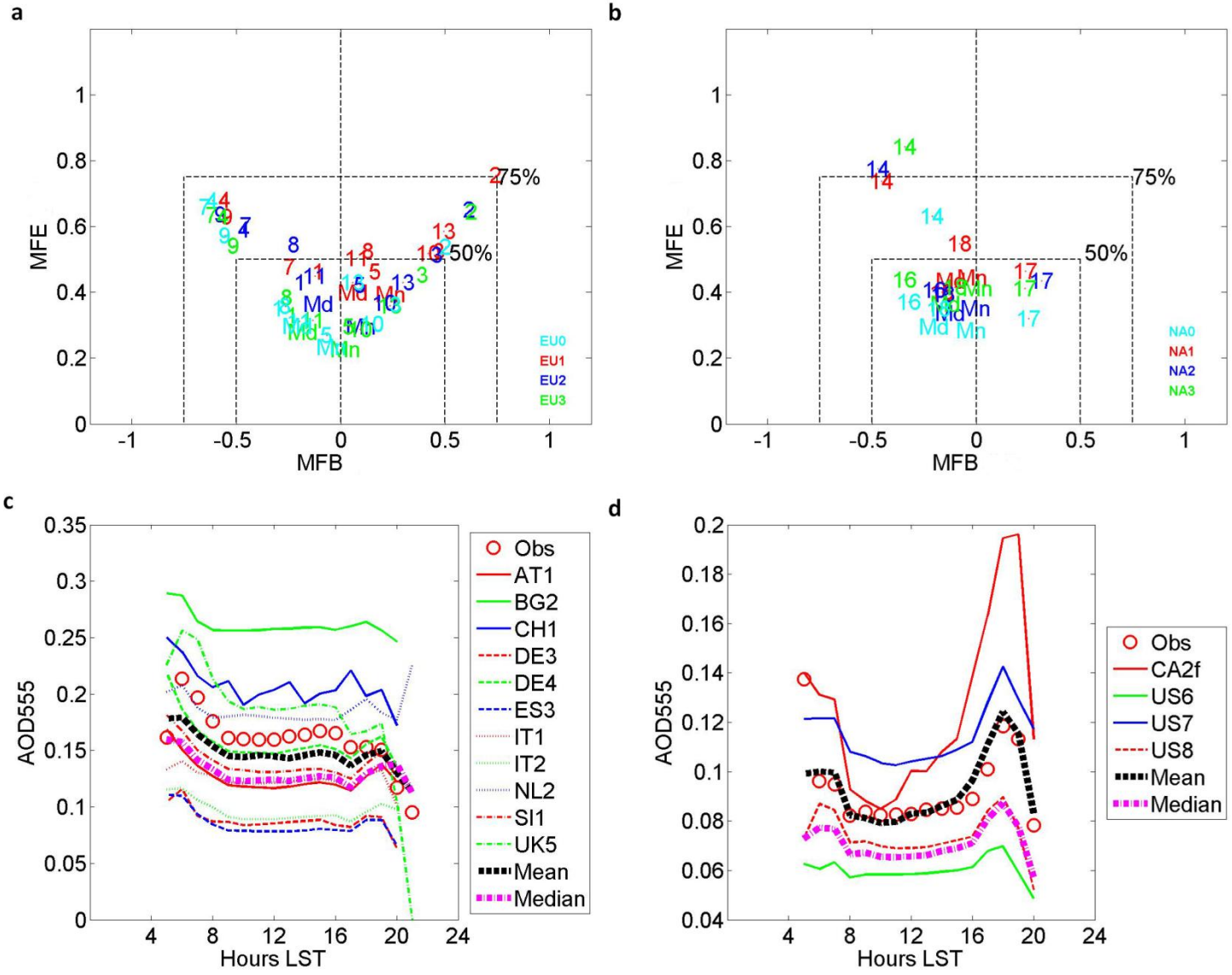
a
b
c
d
MFE
MFB
75%
50%
EU0
EU1
EU2
EU3
NA0
NA1
NA2
NA3
AOD555
Hours LST
Obs
AT1
BG2
CH1
DE3
DE4
ES3
IT1
IT2
NL2
SI1
UK5
Mean
Median
CA2f
US6
US7
US8

Fig.13

Supplementary Material

Click here to download Supplementary Material: Im_etal_PMcollective_SuppMat.docx